frontiers | Frontiers in Marine Science

TYPE Original Research
PUBLISHED 01 December 2022
DOI 10.3389/fmars.2022.1025502

OPEN ACCESS

EDITED BY
Selvaraj Kandasamy,
Xiamen University, China

REVIEWED BY
Manab Kumar Dutta,
National Centre for Earth Science Studies, India
Gvm Gupta,
Centre for Marine Living Resources and Ecology (CMLRE), India
Chen-Tung Arthur Chen,
National Sun Yat-sen University, Taiwan

*CORRESPONDENCE
Sumei Liu
sumeiliu@ouc.edu.cn

SPECIALTY SECTION
This article was submitted to Marine Biogeochemistry, a section of the journal Frontiers in Marine Science

RECEIVED 23 August 2022
ACCEPTED 14 November 2022
PUBLISHED 01 December 2022

CITATION
Liang W, Wang Y, Liu S, Wang M, Zhao L, Liu C, Zhang X, Wu N, Wang L, Zhu D, Ma Y and Luo C (2022) Nutrient dynamics and coupling with biological processes and physical conditions in the Bohai Sea. *Front. Mar. Sci.* 9:1025502. doi: 10.3389/fmars.2022.1025502

Nutrient dynamics and coupling with biological processes and physical conditions in the Bohai Sea

Wen Liang[1,2], Yun Wang[1,2], Sumei Liu[1,2]*, Mengxue Wang[1,2], Liang Zhao[3], Chongcong Liu[1,2], Xiaotong Zhang[1,2], Nian Wu[1,2], Lingyan Wang[1,2], Dongdong Zhu[1,2,4], Yuwei Ma[1,2] and Chang Luo[1,2]

[1]Frontiers Science Center for Deep Ocean Multispheres and Earth System, and Key Laboratory of Marine Chemistry Theory and Technology, Ministry of Education, Ocean University of China, Qingdao, China, [2]Laboratory for Marine Ecology and Environmental Science, Qingdao National Laboratory for Marine Science and Technology, Qingdao, China, [3]College of Marine and Environmental Sciences, Tianjin University of Science and Technology, Tianjin, China, [4]University of Brest, Centre national de la recherche scientifique, L'Institut de recherche pour le développement, Ifremer, Institut Universitaire Européen de la Mer, Plouzané, France

The Bohai Sea is a habitat for economically important fish in China, but its ecological environment has changed significantly, and it is necessary to further clarify the dynamics and the internal resupply channels of nutrients in the Bohai Sea. Based on four field observations in the Bohai Sea from May to December 2019, the nutrient dynamics were addressed. The concentration of dissolved inorganic nutrients was depleted throughout the water column in spring and in the euphotic zone in summer and accumulated in the bottom water in summer and in the water column in autumn and winter. Relative phosphorus limitation was present in Laizhou Bay and its surrounding area in all seasons, while relative silicon limitation was evident in spring and relative nitrogen limitation was significant in summer in most other study aeras. The results of end-member mixing model illustrated significant seasonal differences in the nutrient uptake ratios, which may be related to various factors such as different phytoplankton composition and phosphorus turnover rates. Turbulent entrainment was an important nutrient pathway for primary production in the euphotic zone of Central Bohai Sea during the stratification season, with an estimated average nutrient flux of 6.04 ± 9.63, 0.22 ± 0.19 and 6.97 ± 6.61 mmol·m^{-2}·d^{-1} for DIN, DIP and DSi, respectively.

KEYWORDS

nutrients, end-member mixing model, phytoplankton, turbulent entrainment, Bohai Sea

1 Introduction

Dissolved inorganic nutrients including nitrate (NO_3^-), nitrite (NO_2^-), ammonium (NH_4^+), dissolved inorganic phosphorus (DIP) and dissolved silicate (DSi) are essential nutrients for the growth of phytoplankton (Tyrrell, 1999), which are the basis of the marine food web (Bristow et al., 2017). It has been indicated that dissolved organic nitrogen (DON) may also be an important nitrogen source for the growth of some bacteria or phytoplankton (Shi et al., 2015; Zhang et al., 2015), and dissolved organic phosphorus (DOP) can also be used as an alternative phosphorus source to meet the growth of phytoplankton when DIP concentration is particularly low (Zhang et al., 2019; Fitzsimons et al., 2020). However, due to the rapid population growth and strong anthropogenic activities (e.g. excessive fertilization, fossil fuel combustion, sewage discharge, and water conservancy projects), the global N and P cycles have surpassed the planetary boundaries (RockstrÖm et al., 2009; Steffen et al., 2015). Excessive nutrient inputs can lead to eutrophication in estuaries, bays and marginal seas near the densely populated and economically developed areas, such as the Baltic Sea, Chesapeake Bay, Seto Inland Sea, North Sea and Adriatic Sea (Riegman et al., 1992; Barmawidjaja et al., 1995; Kemp et al., 2005; Ichiro et al., 2006; Voss et al., 2011), thus, can result in the change of phytoplankton community structure (Yunev et al., 2007).

The Bohai Sea, a semi-enclosed marginal sea surrounded by the most densely populated and economically developed terrestrial catchments, is the habitat of economically important fish and the largest mariculture base in China. In the past few decades, the nutrient concentrations and stoichiometric nutrient ratios in the Bohai Sea have been changed significantly, with dissolved inorganic nitrogen (DIN) concentration and DIN/DIP ratio increasing, DIP concentration and DSi/DIN ratio decreasing, and DSi concentration and DSi/DIP ratio first decreasing and then trending upward until the end of 1980s (Liu et al., 2008; Ning et al., 2010; Wang et al., 2019a; Xin et al., 2019). The nutrient limitation for phytoplankton growth changed from nitrogen to phosphorus during the 1980s and 1990s, and then to phosphorus and silicon limitation in the 21st century (Zhang J. et al., 2004; Ning et al., 2010; Liu et al., 2011; Wang et al., 2019a; Xin et al., 2019). Changes in nutrient exacerbated various environmental problems, such as the emergence of succession of phytoplankton, harmful algal blooms, jellyfish blooms and seasonal hypoxia (Wang et al., 2009; Dong et al., 2010; Zhang et al., 2012; Song et al., 2016; Wu et al., 2017; Zhao H.D et al., 2017; Wang et al., 2018; Zhai et al., 2012; Zhai et al., 2019; Han et al., 2019; Luan et al., 2018; Song et al., 2020). Recent studies have also shown that chlorophyll *a* (Chl-*a*) concentrations in the Central Bohai Sea have changed from the previous two peaks in spring and autumn to one peak in spring-summer since 2002 (Ding et al., 2020), with a consistent spatial increase from 2000 to 2012 and then a decrease from 2012 to 2018 (Zhang et al., 2017; Zhai et al., 2021).

The rapid changes in the ecological environment of the Bohai Sea necessitate further clarification of the dynamics of nutrient, which are important for local food webs. In addition, there is a lack of studies on the coupling of phytoplankton with the seasonal variation of nutrients in the Bohai Sea. Furthermore, the concentration of Chl-*a* of Central Bohai Sea has the characteristic of persistently relative high value (Ding et al., 2020), implying a persistently high consumption of nutrients in the euphotic zone during the stratification season, which should be examined. Although results from a three-dimensional coastal shelf sea model - HAMSOM and the direct turbulence observations indicate strong turbulent mixing in winter and weak turbulent mixing in summer in the Bohai Sea (Zhao and Wei, 2001; Xu et al., 2020), the combined turbulent entrainment caused by tides and winds has still been shown to produce weak seawater exchange across the thermocline (Yang et al., 1991). Therefore, during the stratification period, the nutrient fluxes *via* weak turbulent entrainment from the bottom water into the euphotic zone in Central Bohai Sea, where it is less affected by riverine inputs, are worth investigating.

Based on the large observation data of spring, summer, autumn and winter in 2019, spatial and temporal variations of nutrient concentrations in the Bohai Sea were reported in this study, and the coupling of biological processes with the seasonal variations of nutrients was assessed *via* an end-member mixing model. Furthermore, the transport flux of nutrients to the upper ocean *via* turbulent entrainment during stratification season was estimated using a two-layer thermocline model described by Stigebrandt (1981) and compared with atmospheric input.

2 Material and methods

2.1 Oceanographic setting of the study area

The Bohai Sea is a typical semi-enclosed sea with an area of about 77, 000 km^2 and an average water depth of 18 m. The Bohai Sea is divided into Laizhou Bay, Bohai Bay, Liaodong Bay and Central Bohai Sea, and is connected with the Yellow Sea through the narrow Bohai Strait (Figure 1). There is a shallow ridge in Central Bohai Sea, which is 5-10 m shallower than the surrounding waters. A total of 55 rivers flow into the Bohai Sea, with the Yellow River accounting for more than 75% of the total freshwater discharge (Liu et al., 2011). Influenced by the East Asian Monsoon system (Huang et al., 2012), the circulation presents seasonal variation (Figure 1), with basin scale cyclonic circulation in summer and cyclonic circulation in the southern Bohai Sea and anticyclonic circulation in the northern Bohai Sea in winter (Fang et al., 2000; Zhou et al., 2017). The residence time of water in the Bohai Sea is usually more than 1 year (Li et al., 2015; Lin et al., 2020), with poor water exchange capacity and limited self-purification capability. In general, the water exchange

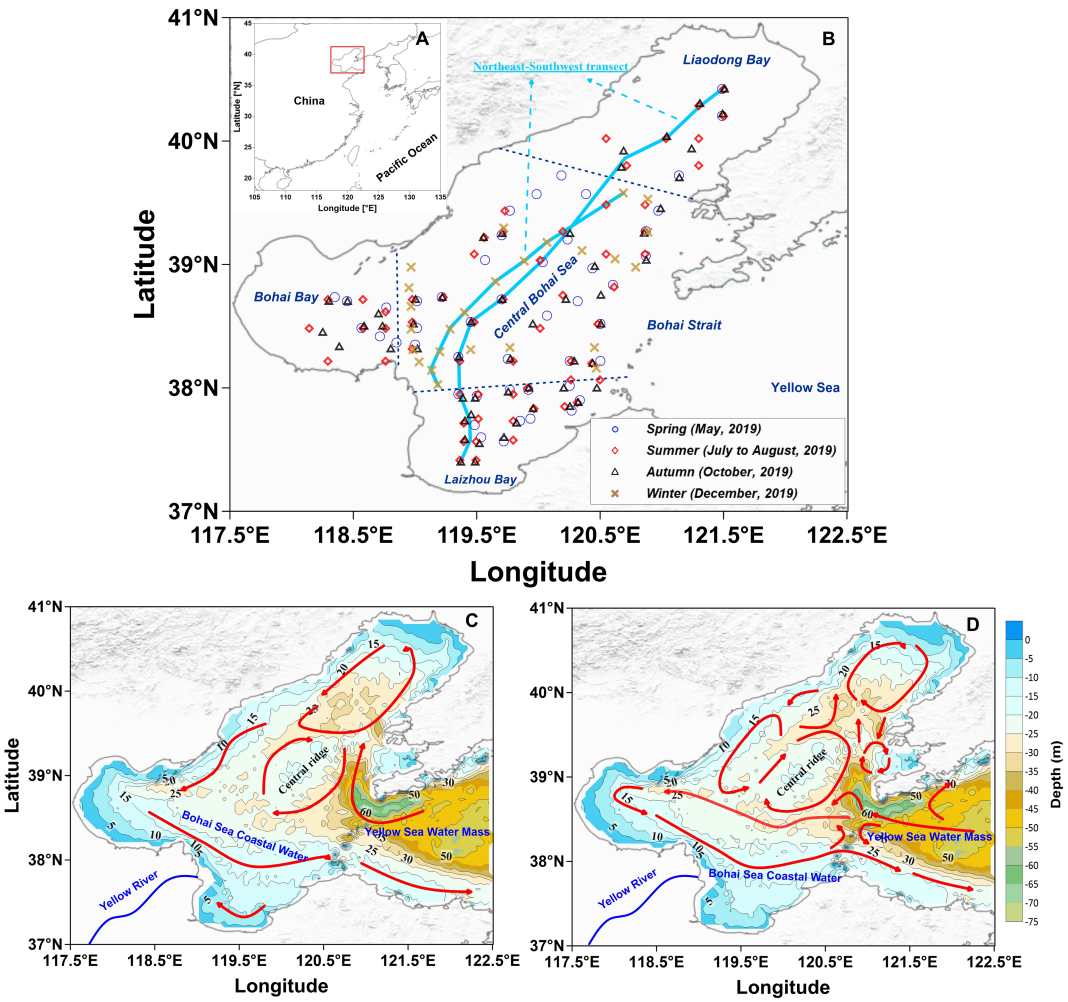

FIGURE 1
Maps showing the geography zoning of the Bohai Sea **(A)**, sampling stations **(B)**, summer circulation **(C)** and winter circulation **(D)**. The summer circulation and winter circulation are redrawn from Zhou et al. (2017) and Fang et al. (2000), respectively. The bold solid lines in sky blue **(A)** represents the Northeast-Southwest transect stations.

between the Bohai Sea and the Yellow Sea in summer and winter were represented by the outflow from the southern strait and the inflow from the northern strait into the Bohai Sea (Luo, 2020).

2.2 Sample collection

In this study, four field observations were conducted in May (spring), July to August (summer), October (autumn) and December (winter) 2019, respectively (Figure 1). The observation stations covered almost the entire Bohai Sea in spring, summer and autumn, while they were mainly concentrated in Central Bohai Sea in winter. Seawater samples of surface (2-3 m), intermediate (1/2 of the seawater depth) and bottom (2 m from the seabed) layers were collected with Niskin hydrophore fitted with a SBE 19 Plus conductivity–temperature–depth (CTD) recorder, which also was equipped with a fluorescent sensor. Seawater used for nutrient analysis were filtered with 0.45 μm polycarbonate membrane, both the filtrate and filters were then frozen at -20°C until they were later analyzed for nutrients and Chl-*a* in the laboratory (Parsons et al., 1984), respectively.

2.3 Nutrient analysis

Concentrations of NO_2^-, NO_3^-, DIP, and DSi were determined with a QuAAtro Continuous Flow Analytical System to measure with the colorimetric methods described by Grasshoff et al. (1999). The detection limits were 0.01 μmol·L^{-1} for NO_3^-, 0.01 μmol·L^{-1} for NO_2^-, 0.01 μmol·L^{-1} for DIP and 0.04 μmol·L^{-1} for DSi, respectively, with the precision< 2%. NH_4^+ was manually measured with a spectrophotometer by the sodium

hypobromate oxidation method, and the detection limit was 0.03 μmol·L^{-1}, with the precision< 3% (Holmes et al., 1999). DIN is the sum of NO_3^-, NO_2^- and NH_4^+. Total dissolved nitrogen (TDN) and total dissolved phosphorus (TDP) were measured using alkaline potassium persulfate oxidation method (Grasshoff et al., 1999). The detection limits of this method were 0.15 μmol·L^{-1} for TDN and 0.03 μmol·L^{-1} for TDP respectively, with the precision less than 5%. DON and DOP concentrations were defined as the respective differences between TDN and DIN, and between TDP and DIP, respectively (Liu et al., 2012).

2.4 Chl-*a* analysis

Concentrations of Chl-*a* were measured following the acetone extraction fluorometric determination method described by Parsons et al. (1984). Firstly, the fluorimeter needed to be calibrated using a known concentration of standard Chl-*a* and 90% acetone solution before measuring the particulates trapped by polycarbonate membrane filters. The fluorescence values of standard Chl-*a* before (R_2) and after acidification (R_1) with 5% (v/v) HCl were measured separately by Turner Designs Trilogy Laboratory fluorimeter, to obtain theacidification factor R (the ratio of R_2 to R_1). Then, the particulates trapped by polycarbonate membrane filters were transferred into a 15 ml polypropylene centrifuge tube. After that, 10 ml of 90% acetone solvent was added to extract it in the dark, at 4°C for 24 h. After the extraction, the tube was centrifugated, and the fluorescence of the clear supernatant solution was measured before and after acidification with 5% (v/v) HCl by fluorimeter following the standard procedure. The excitation wavelength and the emission wavelength were 436 nm and 670 nm, respectively, while the precision was 3.4%. The Chl-*a* concentration of the sample was calculated as:

$$C_{Chl-a} = \frac{R}{R-1}(R_b - R_a)\frac{v}{V} \quad (1)$$

where $C_{Chl\text{-}a}$ is the Chl-*a* concentration (μg·L^{-1}); R is the acidification factor; R_b is the fluorescence value of the sample before acidification; R_a is the fluorescence value of the sample after acidification; v is the volume of the acetone solvent (ml); V is the volume of the filtered sample (L).

2.5 Three end-member mixing model

In this study, a three end-member mixing model was used to differentiate the physically induced changes in nutrients from the biological activities (Han et al., 2012; Wang et al., 2014; Liu S. M.et al., 2017). The model was based on the mass balance equation of potential temperature (θ), salinity (S) and various water mass fractions:

$$\theta = \theta_1 f_1 + \theta_2 f_2 + \theta_3 f_3 \quad (2)$$

$$S = S_1 f_1 + S_2 f_2 + S_3 f_3 \quad (3)$$

$$1 = f_1 + f_2 + f_3 \quad (4)$$

where θ_1, θ_2, and θ_3 are the potential temperature of the three end-members; S_1, S_2, and S_3 are the salinity of the three end-members; θ and S are the potential temperature and salinity in the samples; f_1, f_2 and f_3 are the fractions of each end-member at different samples. The definition of the three end-members for different seasons in this study are given in Section 4.2.1.

The conservative mixing nutrient concentration (N_{mixing}) can be defined as:

$$N_{mixing} = N_1 f_1 + N_2 f_2 + N_3 f_3 \quad (5)$$

where N_1, N_2 and N_3 are the nutrient concentrations of the three end-members.

The difference of nutrient concentration between N_{mixing} and field observation ($N_{measure}$) was represented by ΔN:

$$\Delta N = N_{mixing} - N_{measure} \quad (6)$$

Positive "+" indicates the nutrient consumption, and negative "-" indicates the nutrient production. The uncertainties of nutrient deviation at stations caused by the uncertainty of three end-member parameters are estimated by error propagation formulas (Taylor, 1997).

2.6 Euphotic zone depth

Theoretically, assuming that the water column is homogenous, euphotic zone (Z_{eu}) depth is related to the diffuse attenuation coefficient at 490 nm (Kd(490)) through the following empirical equation (Li et al., 2003):

$$Z_{eu} = 3.512/K_d(490) \quad (7)$$

where $K_d(490)$ is the diffuse attenuation coefficient at 490 nm, derived from MODIS-Aqua (https://oceancolor.gsfc.nasa.gov/l3/order/).

2.7 Mixed layer depth

Based on a density-based criteria (Glover and Brewer, 1988; Kara et al., 2000; Zhao H. D. et al., 2017), the MLD is defined as the depth at which density (ρ) change by a given threshold value (ΔT=0.8°C), relative to the one at a reference depth of 1 m:

$$\rho_{MLD} = \rho(S_{Ref}, T_{Ref} - 0.8, P) \quad (8)$$

where ρ_{MLD} is the density for the MLD, S_{Ref} and T_{Ref} are the salinity and temperature at the reference depth, and P is the reference pressure.

2.8 Calculation of the nutrient flux transported *via* the turbulent entrainment in summer

The entrainment velocity (W_{e1}) from the lower mixed layer to the upper mixed layer during the stratification season can be calculated using a two-layer thermocline model described by Stigebrandt (1981):

$$W_{e1} = 2m_w u_{*w}^3/[ga(T_1 - T_2)h_1] - Q_{in}/[\bar{\rho}C_p(T_1 - T_2)] \quad (9)$$

where m_w is a constant; g is the acceleration of gravity; a is the coefficient of thermal expansion; T_1 and h_1, T_2 and h_2 are the temperature and the depth of the upper and lower mixed layer, respectively; Q_{in} is the net mean heat flow into the sea through the air-sea interface; $\bar{\rho}$ is the average density of seawater; C_p is the specific heat at constant pressure of seawater; u_{*w} is the friction velocity in the upper layer and can be calculated from the wind speed by the well-known relationship $u_{*w}^2 = \rho_a C_{dw} W^2/\bar{\rho}$ (where ρ_a is the density of air; C_{dw} is the appropriate drag coefficient; W is the sea surface wind speed). Part parameter values refer to (Yang et al., 1991; Wei et al., 2002) as follows: m_w=1.2, g = 9.8 m·s^{-2}, a= 3×10^{-4} °C^{-1}, $\bar{\rho}$ =1.021×10^3 kg·m^3, C_p= 3930 J·kg^{-1}·°C^{-1}, ρ_a =1.18 kg·m^{-3}, C_{dw}=1.6×10^{-3}. The W is 4.9 m·s^{-1} (Zhang et al., 2011), while Q_{in} is 193.5 w·m^{-2} in summer (Ren et al., 1990).

Therefore, the vertical nutrient flux transported by turbulent entrainment. (F_t) can be estimated as follows:

$$F_t = W_{e1} C_{deep} \quad (10)$$

where C_{deep} are the nutrient concentrations in the deep water.

3 Results

3.1 Hydrodynamic environment variations

Salinity varied from 25.01 to 32.57 in spring, from 26.30 to 32.39 in summer, from 25.56 to 32.30 in autumn and from 29.26 to 32.37 in winter, showing low values in Laizhou Bay and high values in Liaodong Bay in all seasons (Figures 2–5). Salinity was vertically homogenous in spring, autumn and winter, while the sea surface salinity (average: 30.43 ± 1.86) was slightly lower than the sea bottom salinity (average: 31.37 ± 0.99) in summer, which was associated with the increased freshwater discharge.

The seasonal variation of seawater temperature was consistent with the meteorological characteristics of the Bohai Sea, i.e., temperatures gradually increased from spring (7.51°C to 15.51° C) to summer (17.16°C to 29.53°C), and then decreased in autumn (16.13°C to 19.90°C) and winter (6.94°C to 10.14°C) (Figures 2–5). Seawater temperature was vertically homogenous in spring, autumn and winter. However, low temperature water less than 20°C was found in bottom water in summer, showing temperature-driven seasonal water stratification (Zhou et al., 2009; Zhao H. D, et al., 2017). Notably, the stratification in the shallow ridge of Central Bohai Sea was relatively weak and a well-mixed warm water column was presented (Figure 3). This phenomenon has been reported in several previous studies and was suggested to be associated with the presence of mesoscale anticyclonic eddy in this area in summer (Lin et al., 2006; Zhou et al., 2017; Wei et al., 2019).

Based on the distribution characteristics of potential temperature, salinity and the geographical location of sampling stations in the Bohai Sea from spring to winter, we simply distinguished the water masses, i.e. the Yellow River Diluted Water (YRDW), Bohai Sea Coastal Water (BSCW), Bohai Sea Water Mass (BSWM) and Yellow Sea Water Mass (YSWM) (Figure 6). It should be noted that the YSWM was subdivided into Surface-YSWM and Bottom-YSWM in summer due to the influence of stratification.

The MLD in summer had the similar distribution characteristics with temperature, with the MLD less than 4 m in most areas, but penetrating to the seafloor in nearshore areas and central ridge (Figure 7). In the rest seasons, the MLD at almost all stations penetrated to the seafloor due to the well vertical mixing of seawater (not shown).

In general, the depth of Z_{eu} in the inshore (< 12 m) was lower than that in Central Bohai Sea (12-20 m) (Figure 8). The depth of Z_{eu} in the Yellow River Estuary was slightly shallower in summer than in other seasons due to the increase of river discharge, but the depth of Z_{eu} in Central Bohai Sea and southern Liaodong Bay was deeper in summer than that in other seasons. In addition, there were no significant seasonal differences in the depth of Z_{eu} in spring, autumn and winter.

3.2 Nutrients from spring to winter in 2019

The distribution of nutrient concentrations (DIN, DIP, DON, DOP and DSi) at surface layer and Northeast-Southwest transect for each season were shown in Figures 2–5. The surface and transect distributions of NO_3^-, NO_2^- and NH_4^+ concentrations were placed in Supplementary Figure 1 and Supplementary Figure 2, respectively. The nutrient concentrations and structures in different regions were shown in Supplementary Table 1.

3.2.1 Nutrients in spring

During the spring cruise, the average nutrient concentrations were 4.97 ± 6.13 μmol·L^{-1} for NO_3^-, 0.09 ± 0.09 μmol·L^{-1} for NO_2^-, 1.21 ± 0.78 μmol·L^{-1} for NH_4^+, 6.28 ± 6.43 μmol·L^{-1} for DIN, 22.78 ± 7.22 μmol·L^{-1} for DON, 0.14 ± 0.06 μmol·L^{-1} for DIP, 0.58 ± 0.30 μmol·L^{-1} for DOP and 1.38

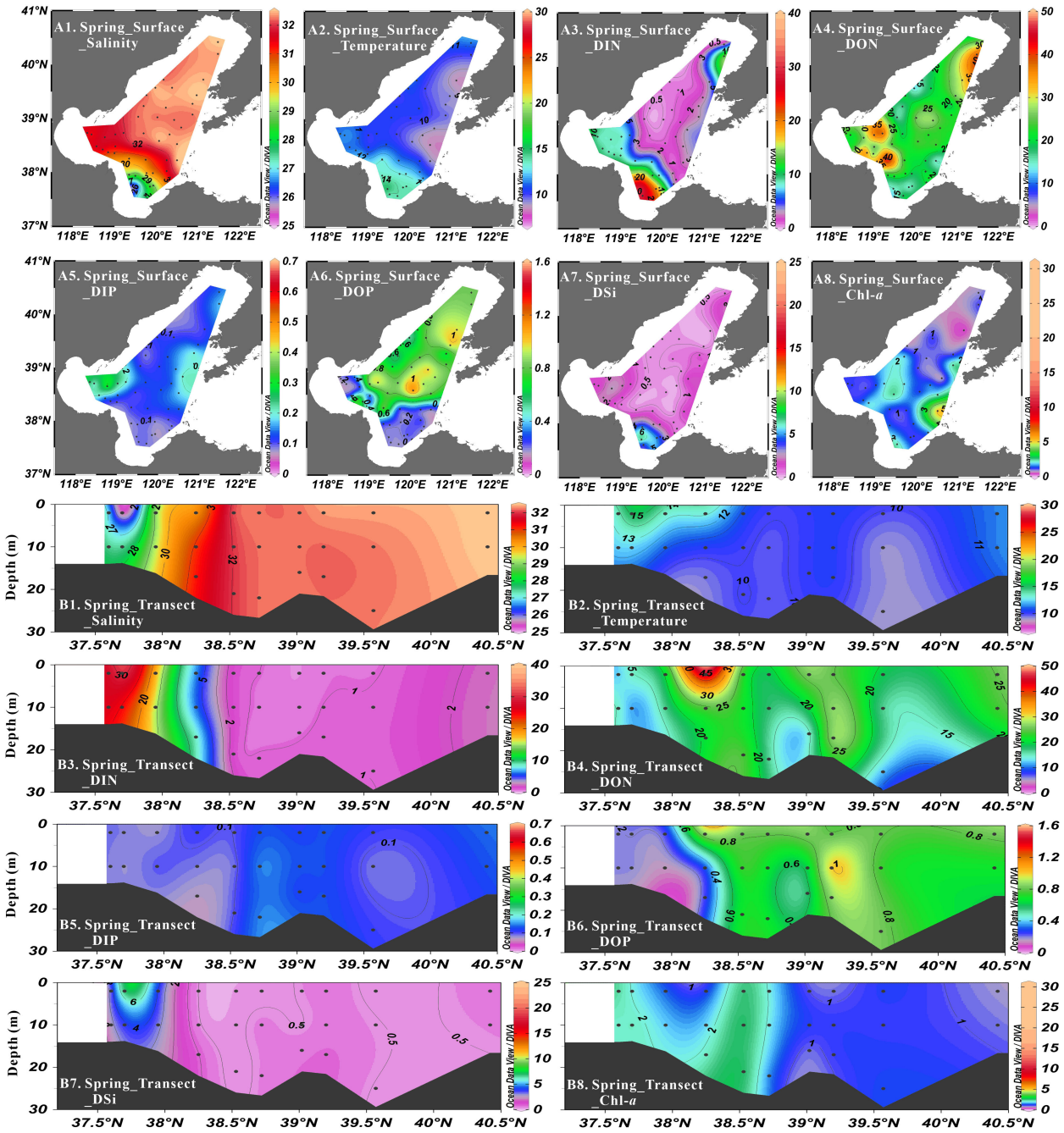

FIGURE 2
Distribution of salinity (psu), temperature (°C), DIN concentration (μmol·L^{-1}), DON concentration (μmol·L^{-1}), DIP concentration (μmol·L^{-1}), DOP concentration (μmol·L^{-1}), DSi concentration (μmol·L^{-1}) and Chl-*a* concentration (μg·L^{-1}) at surface layer (A1-A8) and Northeast-Southwest transect (B1-B8) in spring.

± 1.28 μmol·L^{-1} for DSi. The nutrient concentrations were vertically uniform due to vertically well-mixed seawater. In terms of regional distribution, the concentrations of NO_3^- (0.00-29.75 μmol·L^{-1}), NO_2^- (0.00-0.41 μmol·L^{-1}), NH_4^+ (0.04-4.89 μmol·L^{-1}), DIN (0.08-31.74 μmol·L^{-1}) and DSi (0.16-7.57 μmol·L^{-1}) decreased from the coastal areas to Central Bohai Sea. The DON concentrations were higher in northern Liaodong Bay and Bohai Bay (> 30 μmol·L^{-1}) than in other areas. High values

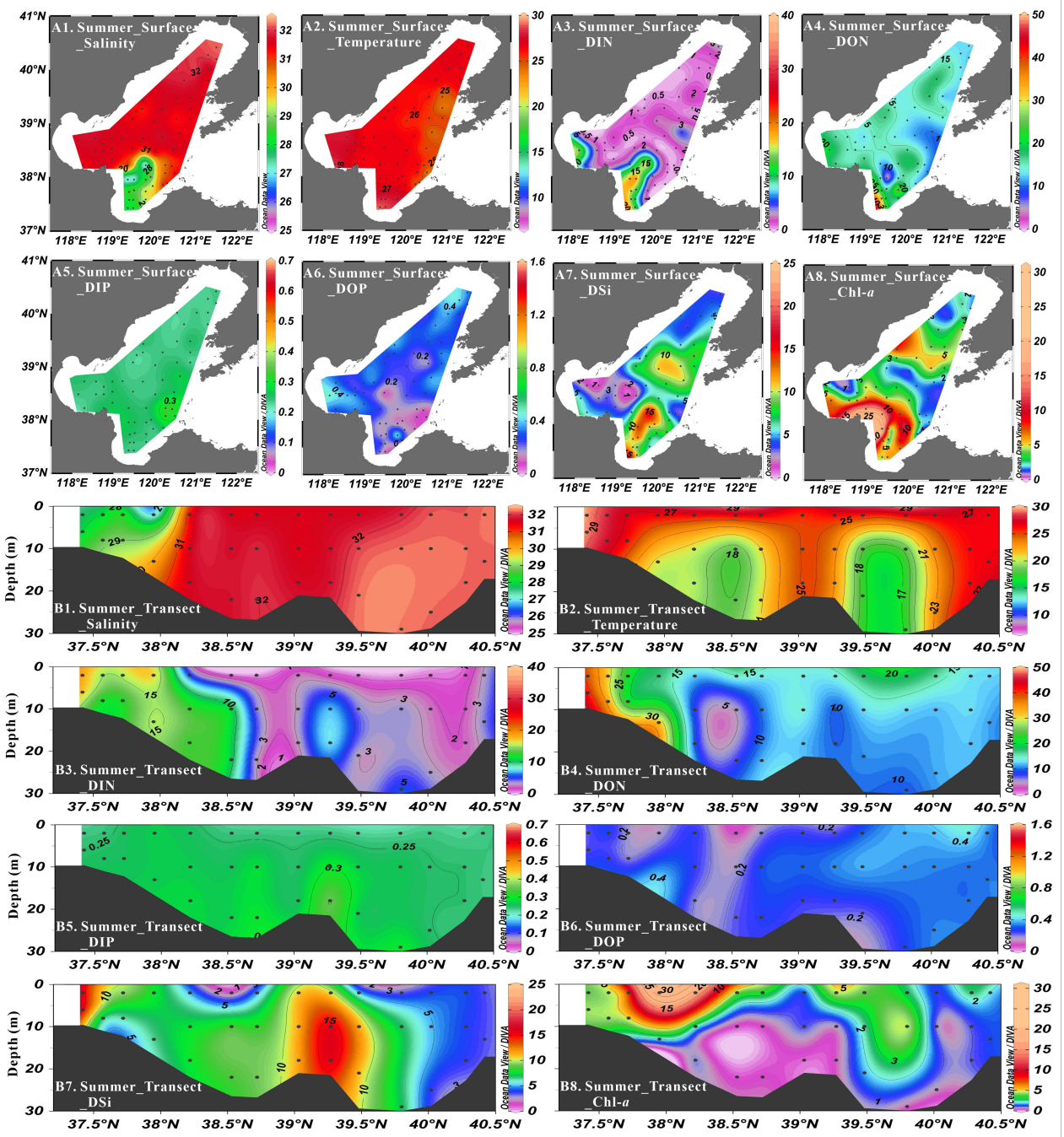

FIGURE 3
Distribution of salinity (psu), temperature (°C), DIN concentration (μmol·L^{-1}), DON concentration (μmol·L^{-1}), DIP concentration (μmol·L^{-1}), DOP concentration (μmol·L^{-1}), DSi concentration (μmol·L^{-1}) and Chl-*a* concentration (μg·L^{-1}) at surface layer (A1-A8) and Northeast-Southwest transect (B1-B8) in summer.

of DIP concentrations (> 0.2 μmol·L^{-1}) were observed in Bohai Bay and the areas near Bohai Strait, while the lowest values (< 0.1 μmol·L^{-1}) were found in Laizhou Bay. The DOP concentrations decreased from the northeast (0.78 ± 0.16 μmol·L^{-1}) to the southwest (ca. 0.2 μmol·L^{-1}). The DIN/DIP ratios and DSi/DIP ratios varied from 0.7 to 340 and 1.2 to 80.9, respectively, gradually decreasing from the three bays to Central Bohai Sea. On the contrary, DSi/DIN ratios varied from 0.1 to 2.0 and

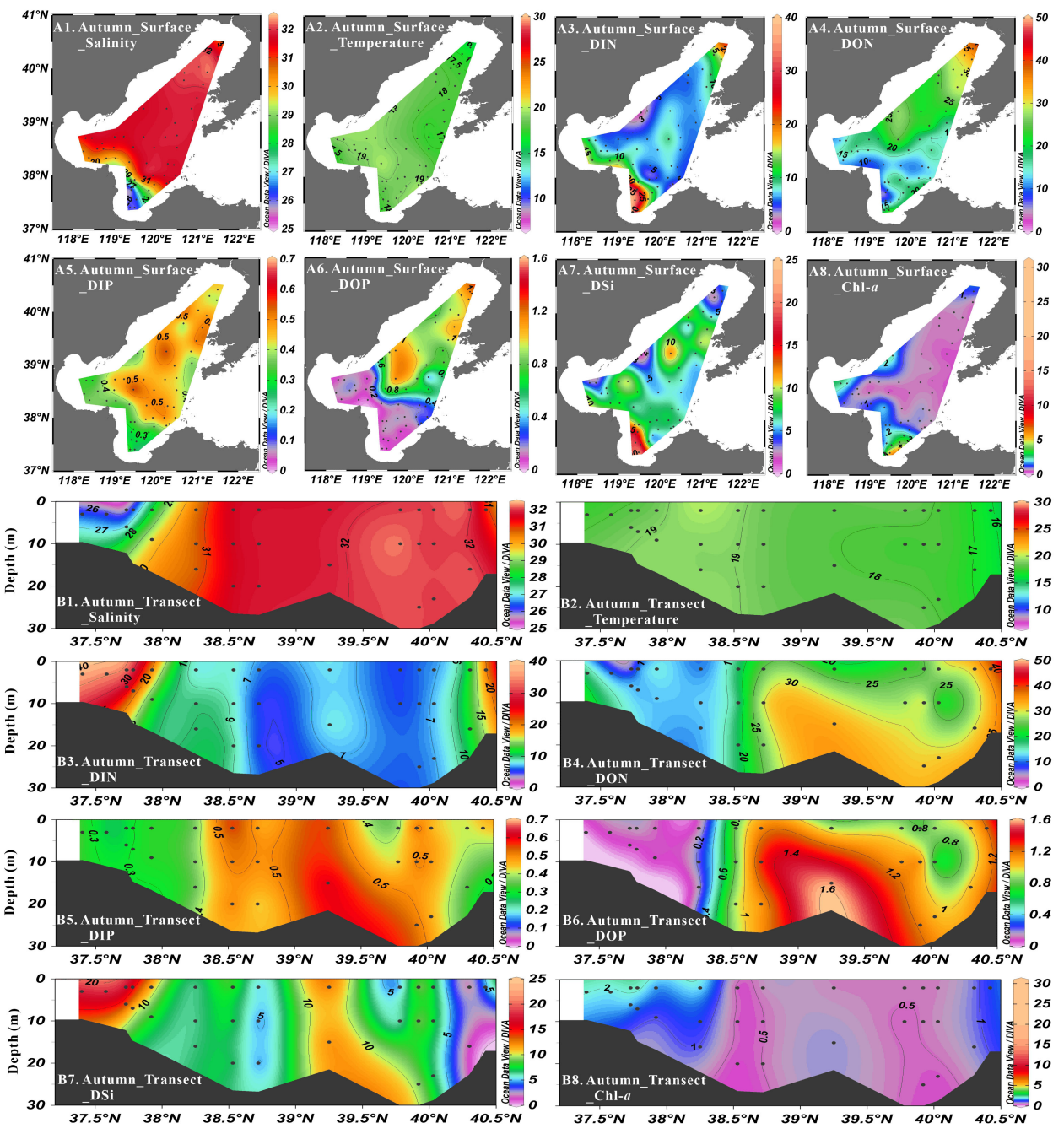

FIGURE 4
Distribution of salinity (psu), temperature (°C), DIN concentration (μmol·L^{-1}), DON concentration (μmol·L^{-1}), DIP concentration (μmol·L^{-1}), DOP concentration (μmol·L^{-1}), DSi concentration (μmol·L^{-1}) and Chl-*a* concentration (μg·L^{-1}) at surface layer (A1-A8) and Northeast-Southwest transect (B1-B8) in autumn.

increased from the three bays to Central Bohai Sea. For nitrogen compounds, NO_3^- contributed to 1–96% (average: 57%) of DIN, then followed by NH_4^+, which contributed to 3–95% (average: 41%) of DIN. NO_2^- occupied the smallest proportion, which was just 0–19% (average: 2%) of DIN. With respect to the composition of TDN, DON was the main form of TDN, accounting for 30-100% (average: 81%) in the whole study area. For phosphorus compounds, DIP and DOP represented 10-65% (average: 23%) and 35–90% (average: 77%) of TDP, respectively.

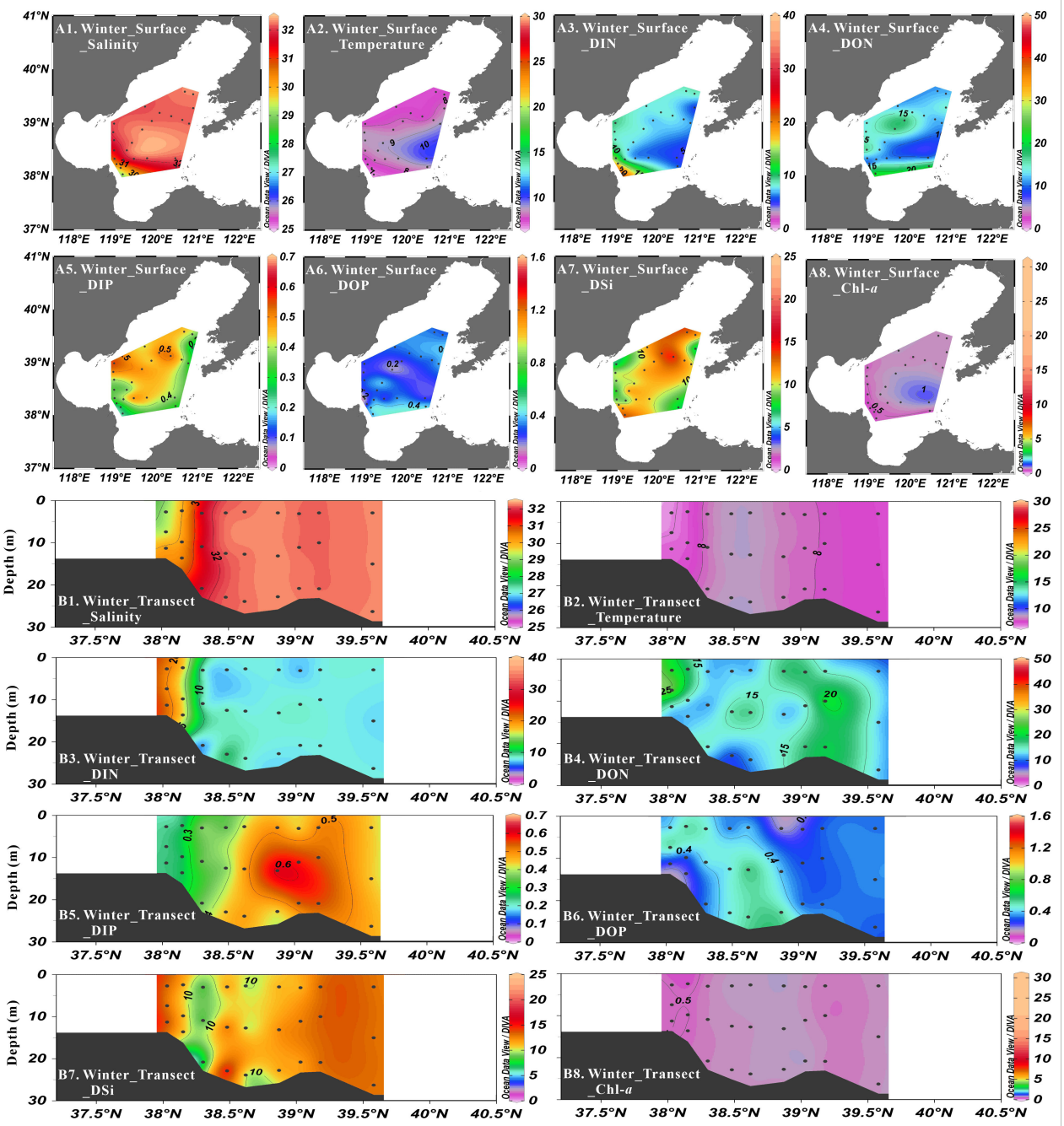

FIGURE 5
Distribution of salinity (psu), temperature (°C), DIN concentration (μmol·L^{-1}), DON concentration (μmol·L^{-1}), DIP concentration (μmol·L^{-1}), DOP concentration (μmol·L^{-1}), DSi concentration (μmol·L^{-1}) and Chl-*a* concentration (μg·L^{-1}) at surface layer (A1-A8) and Northeast-Southwest transect (B1-B8) in winter.

3.2.2 Nutrients in summer

In summer cruise, the average concentrations of nutrients were 1.46 ± 2.45 μmol·L^{-1} for NO_3^-, 0.89 ± 1.02 μmol·L^{-1} for NO_2^-, 2.70 ± 2.68 μmol·L^{-1} for NH_4^+, 5.06 ± 4.94 μmol·L^{-1} for DIN, 14.26 ± 6.83 μmol·L^{-1} for DON, 0.26 ± 0.03 μmol·L^{-1} for DIP, 0.27 ± 0.10 μmol·L^{-1} for DOP and 7.61 ± 3.50 μmol·L^{-1} for DSi. The concentrations of all inorganic nutrients were higher at bottom layer than those at surface layer except in the Yellow River Estuary. The concentration of NO_3^- was very low (< 1 μmol·L^{-1}) at surface layer in Liaodong Bay and most of

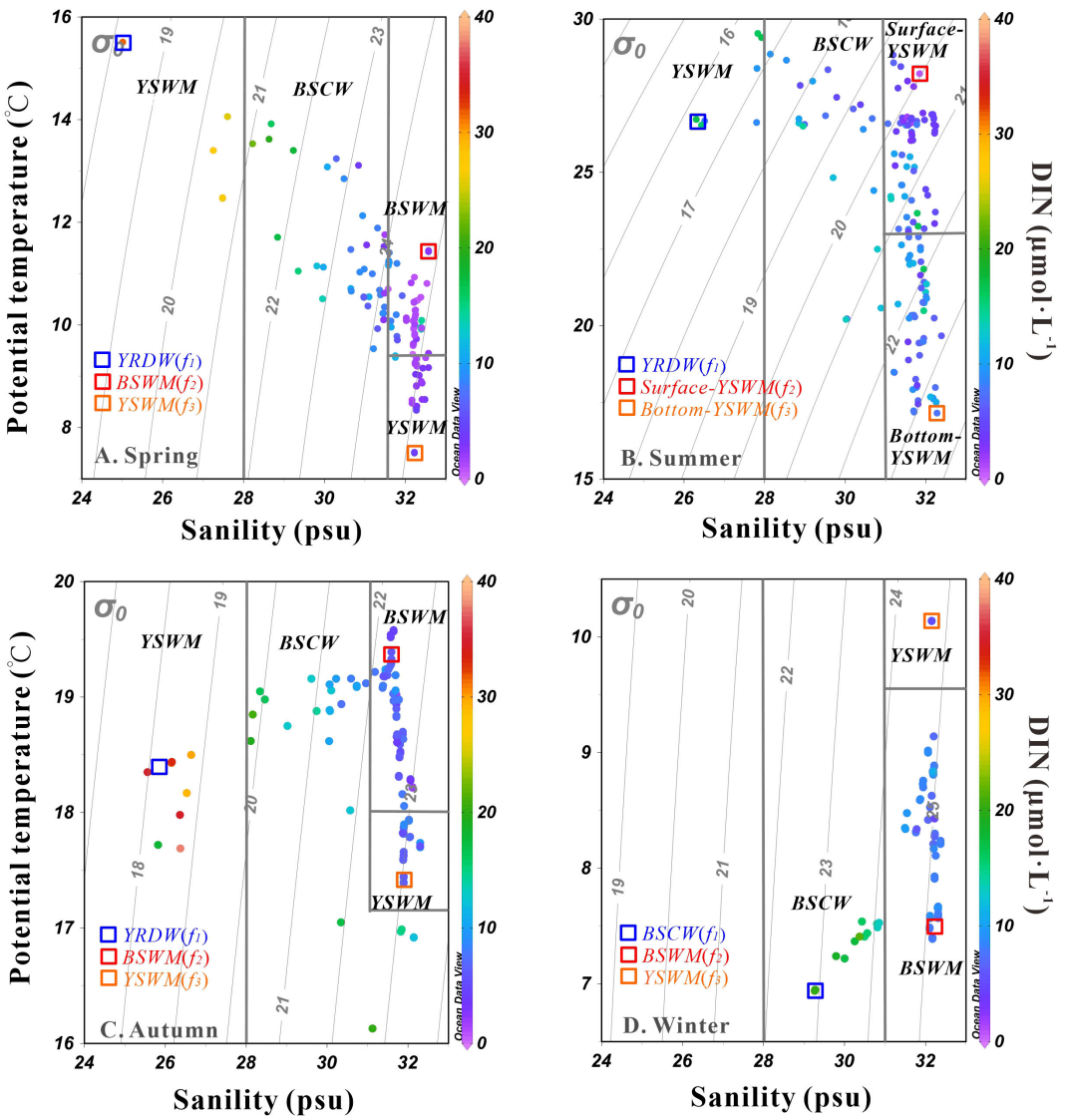

FIGURE 6
The potential temperature (θ) *vs.* salinity scheme in the Bohai Sea in spring **(A)**, summer **(B)**, autumn **(C)** and winter **(D)**, with the color of solid dots representing DIN concentration. End-members are marked with different colored squares.

Central Bohai Sea. The concentrations of NO_3^- (0.00-16.93 μmol·L^{-1}), NH_4^+ (0.12-12.67 μmol·L^{-1}), DIN (0.17-19.88 μmol·L^{-1}) and DON (0.90-47.15 μmol·L^{-1}) increased from the northeast to the southwest, with the highest values observed in Laizhou Bay. The DSi concentrations in Laizhou Bay (9.97 ± 3.13 μmol·L^{-1}) and Central Bohai Sea (8.12 ± 3.58 μmol·L^{-1}) were relatively higher than that in Bohai Bay (4.79 ± 1.93 μmol·L^{-1}) and Liaodong Bay (5.62 ± 2.06 μmol·L^{-1}). The DIP concentrations varied from 0.17 to 0.37 μmol·L^{-1} in the whole study area without obvious geographical characteristics, while the DOP concentrations decreased from the northeast (0.32 ± 0.06 μmol·L^{-1}) to the southwest (0.22 ± 0.13 μmol·L^{-1}). The DIN/DIP ratios ranged from 0.8 to 76.7, showing a gradually decreasing distribution from southwest to northeast. The DSi/DIN ratios ranged from 0.4 to 42.0 and increased from the three bays to Central Bohai Sea. The DSi/DIP ratios varied from 2.8 to 68.4, with relatively higher values observed in Laizhou Bay and Central Bohai Sea. Consistent with the stratification of seawater, the respective compositions of DIN and TDN were different in the vertical direction. NH_4^+, NO_3^- and NO_2^- at surface layer accounted for ca. 48%, ca. 43% and ca. 9% of DIN, respectively. However, NH_4^+, NO_3^- and NO_2^- at bottom layer accounted for ca. 59%, ca. 20% and ca. 21% of DIN, respectively. With respect to the composition of TDN, DON accounted for ca. 81% of TDN

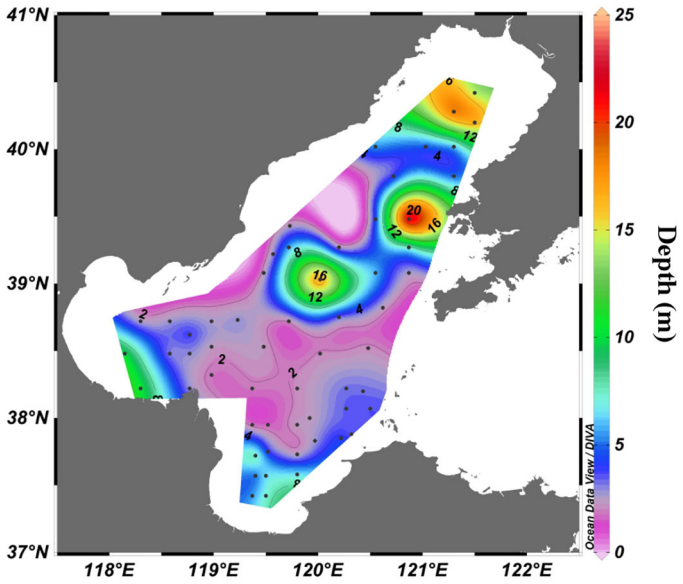

FIGURE 7
The depth of MLD in summer.

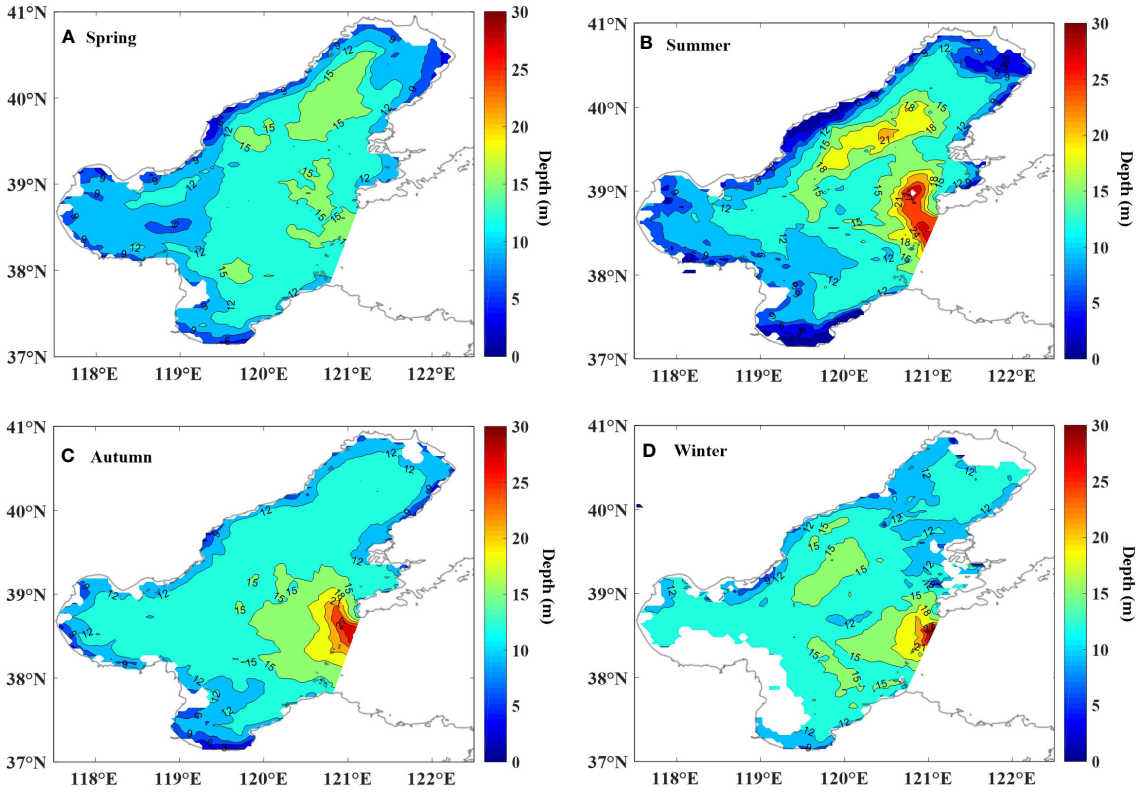

FIGURE 8
The depth of Z_{eu} distribution in spring **(A)**, summer **(B)**, autumn **(C)** and winter **(D)**.

at surface layer and ca. 69% at bottom layer, respectively. For phosphorus compounds, DIP and DOP shared the close contribution proportions, representing ca. 51% and ca. 49% of TDP, respectively.

3.2.3 Nutrients in autumn

In autumn, the average nutrient concentrations were 6.11 ± 6.08 μmol·L^{-1} for NO_3^-, 1.31 ± 1.05 μmol·L^{-1} for NO_2^-, 2.00 ± 1.39 μmol·L^{-1} for NH_4^+, 9.42 ± 6.83 μmol·L^{-1} for DIN, 18.69 ± 7.42 μmol·L^{-1} for DON, 0.41 ± 0.07 μmol·L^{-1} for DIP, 0.48 ± 0.42 μmol·L^{-1} for DOP and 7.38 ± 3.52 μmol·L^{-1} for DSi. Nutrients were homogeneously mixed in the vertical direction. In terms of regional distribution, the concentrations of NO_3^- (0.58-30.18 μmol·L^{-1}) and DIN (1.46-37.73 μmol·L^{-1}) gradual decreased from the three bays to Central Bohai Sea, with the highest values appeared in Laizhou Bay. The high values of NO_2^- (> 2 μmol·L^{-1}) and NH_4^+ (> 3 μmol·L^{-1}) concentrations were observed in Laizhou Bay, Central Bohai Sea and northern Liaodong Bay. The DSi concentration in Laizhou Bay (10.24 ± 5.07 μmol·L^{-1}) was much higher, while the lowest value was found in northern Liaodong Bay and northwestern Central Bohai Sea (< 5 μmol·L^{-1}). The concentrations of DIP (0.24-0.61 μmol·L^{-1}), DOP (0.01-1.59 μmol·L^{-1}) and DON (2.76-37.81 μmol·L^{-1}) decreased from northeast to southwest, with the low values appeared in Bohai Bay and Laizhou Bay. The DIN/DIP ratios and DSi/DIP ratios varied from 4.0 to 126.9 and 3.8 to 94.6, respectively, with a gradual decrease from the three bays to Central Bohai Sea. DSi/DIN ratios ranged from 0.1 to 1.9, increasing from the three bays to Central Bohai Sea. The predominant component of DIN was NO_3^-, accounting for 14-97% (average: 58%), while NH_4^+ was the secondary dominant component, accounting for 0–75% (average: 25%). NO_2^- occupied the smallest proportion, which was just 0–41% (average: 17%) of DIN. DON accounted for 7–95% (average: 67%) of TDN in the whole study area. For phosphorus compounds, DIP and DOP represented 21-93% (average: 57%) and 3-79% (average: 43%) of TDP, respectively.

3.2.4 Nutrients in winter

In winter cruise, the average nutrient concentrations in Central Bohai Sea were 8.85 ± 3.93 μmol·L^{-1} for NO_3^-, 0.23 ± 0.37 μmol·L^{-1} for NO_2^-, 0.31 ± 0.39 μmol·L^{-1} for NH_4^+, 9.39 ± 3.77 μmol·L^{-1} for DIN, 13.70 ± 3.62 μmol·L^{-1} for DON, 0.42 ± 0.10 μmol·L^{-1} for DIP, 0.32 ± 0.13 μmol·L^{-1} for DOP and 10.68 ± 2.33 μmol·L^{-1} for DSi. The concentrations of all inorganic nutrients were vertically homogenous. In terms of regional distribution, the concentrations of NO_3^- (4.58-21.32 μmol·L^{-1}) and DIN (4.89-21.52 μmol·L^{-1}) generally decreased from southwest to northeast. The concentrations of NO_2^- (0.00-1.62 μmol·L^{-1}) and NH_4^+ (0.05-1.79 μmol·L^{-1}) existed higher values in the northwestern Central Bohai Sea and relatively lower values in other regions. The concentrations of DIP generally increased from southwest (~0.3 μmol·L^{-1}) to northeast (~0.5 μmol·L^{-1}). Higher DSi concentrations (> 10 μmol·L^{-1}) were observed in all areas except near the Bohai Strait and Bohai Bay. Higher values of DON (> 15 μmol·L^{-1}) were observed in southern Central Bohai Sea and northwestern Central Bohai Sea, with relatively lower values in other areas. The relatively higher values of DOP concentration were observed in southern Central Bohai Sea. The DIN/DIP ratios and DSi/DIP ratios ranged from 11.2 to 87.8 and 11.6 to 57.0, respectively, decreasing gradually from southwest to northeast. DIN/DSi ratios ranged from 0.6 to 1.9, showing a gradually increasing distribution from southwest to northeast. For nitrogen compounds, NO_3^- contributed to 57–99% (average: 94%) of DIN, while NH_4^+ and NO_2^- shared the similar proportions (average: 3%). In TDN, DON accounted for ca. 60% and DIN accounted for ca. 40% in the whole study area. For phosphorus compounds, DIP and DOP represented ca. 57% and ca. 43% of TDP, respectively.

3.3 Seasonal variation of Chl-*a*

Seasonally, the Chl-*a* concentration was highest in summer, followed by spring, autumn and winter during the investigation periods (Figures 2–5). In spring, the concentration of Chl-*a* ranged from 0.29 to 7.50 (average: 1.58 ± 1.16) μg·L^{-1}, with high value located in Central Bohai Sea and Laizhou Bay and relatively low values in other regions. In summer, the concentration of Chl-*a* ranged from 0.18 to 30.53 (average: 3.02 ± 4.12) μg·L^{-1}, with much higher concentration at surface layer than that at bottom layer. In autumn, the concentration of Chl-*a* varied from 0.34 to 6.47 (average: 0.99 ± 0.80) μg·L^{-1}, with high values observed in Laizhou Bay, Bohai Bay and northwestern Central Bohai Sea compared to other regions. In winter, the concentration of Chl-*a* varied from 0.16 to 1.02 (average: 0.60 ± 0.15) μg·L^{-1} in Central Bohai Sea, with relatively high values at station near the Bohai Strait and relatively low values in other areas.

4 Discussion

4.1 Nutrient regime

High DIN and DSi concentrations in Laizhou Bay and other coastal waters in all seasons were considered to be related to the riverine input (Liu et al., 2009; Liu et al., 2012; Liu, 2015; Wang et al., 2019a; Xin et al., 2019; Wu et al., 2021), wastewater discharge (Wang et al., 2019a), submarine groundwater discharges (Liu J. et al., 2017; Wang et al., 2020) and mariculture effluent (Cui et al., 2005; Wang et al., 2019b). The relationship between nutrients and salinity was statistically analyzed. DIN and DSi concentrations were negatively correlated with salinity ($0.385 \leq r \leq 0.918$, $p < 0.01$, $71 \leq n \leq$

144). It should be noted that there are fewer stations in winter, so it showed that there was no relationship between DSi concentration and salinity, but for the data with salinity less than 31, the negative correlation was significant (r=0.778, $p < 0.01$, n=12). Positive correlation between DIP and salinity ($0.210 \leq r \leq 0.712$, $p < 0.05$) at least suggest that the terrestrial inputs were not the main source of phosphorus. The low DIP concentration in Laizhou Bay was mainly ascribed to the dilution of low DIP concentration of the YRDW itself and the adsorption of DIP by the abundant suspended particulate matter in the river (Pan et al., 2013; Wu et al., 2021).

Significant seasonal changes in nutrients were observed in the Bohai Sea. In winter, the inorganic nutrients in Central Bohai Sea were almost the most abundant throughout the year, which provided a good material basis for the phytoplankton growth in the coming spring. With the coming of early spring, the temperatures and solar radiation begin to increase and the wind stresses diminish, which provides the optimal environmental conditions for phytoplankton growth. Compared with the concentrations of nutrients in winter, the inorganic nutrients in Central Bohai Sea in spring decreased significantly, while organic nutrients increased. This indicated that phytoplankton assimilation was enhanced from winter to spring, corresponding to higher Chl-*a* concentrations in Central Bohai Sea in spring. In particular, DSi concentration and DSi/DIN ratio in Central Bohai Sea decreased sharply from 10.68 ± 2.33 μmol·L^{-1} and 1.3 ± 0.4 in winter to 0.85 ± 0.60 μmol·L^{-1} and 0.4 ± 0.3 in spring, respectively, which should be the result of DSi uptake by siliceous organisms. This speculation was also supported by the phytoplankton population results in spring, with the dominant species being mainly *Paralia sulcate* and *Coscinodiscus* sp. (Yang et al., 2016). Significant relative silicon limitation was present in most areas due to the high nutrient consumption (Figure 9). While significant relative phosphorus limitation was present in Laizhou Bay and its surrounding area in all seasons (Figure 9), which is in agreement with the previous *in-situ* incubation experiments (Turner et al., 1990; Zou et al., 2001; Zhang J. et al., 2004). In the presence of relative silicon limitation, the average abundance of non-siliceous organism accounted for ~49% of the total phytoplankton abundance in Central Bohai Sea (Zhang, 2016a).

From spring to summer, there were still high DIN and DSi concentrations in Laizhou Bay. However, DIN concentrations at surface layer were still very low (< 1 μmol·L^{-1}) in most of the other study areas. While high concentrations of regenerated nitrogen at bottom layer mainly originatedfrom mineralization of organic matter in the sediment (Liu et al., 2011), which corresponded to consumption dissolved oxygen at bottom layer driven by it (Zhao H. D. et al., 2017; Song et al., 2020). Interestingly, the average DIP concentration increased slightly from 0.14 ± 0.06 μmol·L^{-1} in spring to 0.26 ± 0.03 μmol·L^{-1} in summer, with DIP being in excess relative to DIN in most of the study area. The average DSi concentration in the whole study area increased significantly from 1.38 ± 1.28 μmol·L^{-1} in spring to 7.61 ± 3.50 μmol·L^{-1} in summer, which may be related to the fact that siliceous organisms are not adapted to high light and low nutrient environment (see discussion in Section 4.2.2). The nutrient ratios in the most study area was characterized by very higher DSi/DIN ratio, lower DIN/DIP ratio and slightly higher DSi/DIP ratio compared to typical Redfield ratios, implying a significant relative nitrogen limitation in the most study area in summer (Figure 9). However, some stations in Central Bohai Sea still featured high Chl-*a* concentrations under relative nitrogen limitation, suggesting that there are other pathways that may have supported primary production (see discussion in Section 4.3).

From summer to autumn, and then to winter, inorganic nutrient concentrations increased significantly throughout the water column. The nutrient ratios in the study areas were close to the canonical Redfield ratio and in agreement with previous reports (Zheng et al., 2020), with an absence of significant relative nutrient limitation (Figure 9). However, under the condition of sufficient ambient nutrients, the Chl-*a* concentrations in autumn and winter were still lower than that in other two seasons. Similar to the seasonal variation of Chl-*a* concentration, the average phytoplankton abundance in the water samples was significantly lower in autumn (5.25×10^3 cells·L^{-1}) and winter (2.17×10^3 cells·L^{-1}) than in summer (14.6×10^3 cells·L^{-1}) (Hou et al., 2021; Wang et al., 2022), although the Shannon-Wiener index was higher in autumn (2.37) than in other seasons (1.64-1.71) (Hou et al., 2021; Wang et al., 2022). The depth of euphotic zone seemed not to be an influencing factor, as it did not vary significantly seasonally. We suggest that the resistance time of phytoplankton in euphotic zone may be an important factor. Shorter sunshine duration and higher frequency and stronger strength of winds in autumn and winter (Li et al., 2016; Ren et al., 2017) probably reduce the resistance time of phytoplankton in the euphotic zone, thus reduce the biomass (Fu et al., 2016). Also, colder temperatures may be an important factor limiting phytoplankton growth in winter (Sun et al., 2001).

4.2 Nutrient uptake derived from the three end-member mixing model

4.2.1 Selection of end-members and model validation

As mentioned above, biological processes will affect the nutrient dynamics in the Bohai Sea. In this study, a three end-member mixing model was used to analyze the biological activity of the four seasons. In spring and autumn, YRDW, BSWM and YSWM were used as the three end-members. In summer, YRDW, Surface-YSWM and Bottom-YSWM were used as the three end-members. In winter, observations were only carried out in Central Bohai Sea, and three water masses (i.e. BSCW,

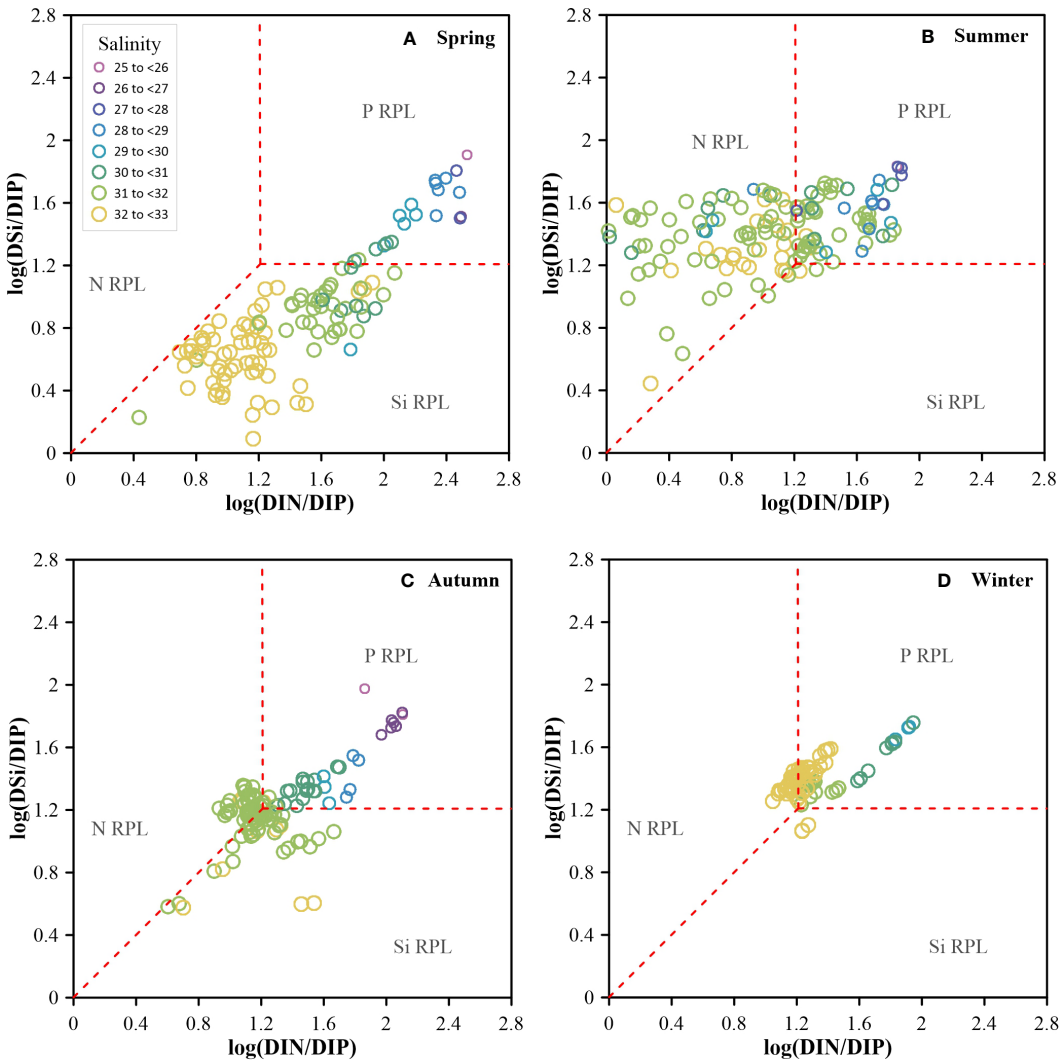

FIGURE 9
Log (DSi/DIP) vs. log (DIN/DIP) in spring **(A)**, summer **(B)**, autumn **(C)** and winter **(D)**. The red dashed line indicates DIN/DIP=16, DSi/DIP=16, and DSi/DIN=1. The rectangular area in the top right represents P Relative Potential Limitation (RPL) area; the lower trapezoidal area represents Si RPL area; and the left trapezoid represents N RPL area.

BSWM and YSWM) were detected. All end-members in each season were marked with different colored squares in Figure 6, and their values were taken from the measured data in this study and can be found in Table 1. The end-member values of YRDW in spring, summer and autumn or BSCW in winter were obtained by single sample or averaging samples from the low salinity stations. The end-member values of BSWM in spring and autumn or Surface-YSWM in summer were obtained by averaging samples or single sample from the high temperature and high salinity stations, and the end-member values of BSWM in winter was obtained by the averaging samples from the low temperature and high salinity stations. The end-member values of YSWM in spring and autumn or Bottom-YSWM in summer were obtained by averaging samples or single sample from the low temperature and high salinity stations, and the end-member values of YSWM in winter was obtained by averaging samples from the high temperature and high salinity stations. Based on the model, the fraction of each end-member contributing to the samples (Figure 10) was calculated to predict conservative mixing values of nutrients.

4.2.2 Nutrient uptake in the euphotic zone from spring to winter

The deviations of nutrient concentrations in the euphotic zone derived from the three end-member mixing model for the four seasons were shown in Figure 11. Positive deviations of

TABLE 1 Summary of the end-member values and their average uncertainties (ε) used in three end-member.

Season	Water mass	Temperature (°C)	Salinity	DIN (μmol/L)	DIP (μmol/L)	DSi (μmol/L)	εΔDIN (μmol/L)	εΔDIP (μmol/L)	εΔDSi (μmol/L)
Spring	YRDW	15.51 ± 0.00	25.01 ± 0.00	31.74 ± 0.00	0.09 ± 0.00	7.57 ± 0.00	0.04	0.01	0.03
	BSWM	11.44 ± 0.02	32.57 ± 0.00	0.76 ± 0.16	0.14 ± 0.01	0.65 ± 0.08			
	YSWM	7.52 ± 0.00	32.22 ± 0.00	3.60 ± 0.84	0.26 ± 0.10	1.72 ± 0.67			
Summer	YRDW	26.65 ± 0.10	26.41 ± 0.10	18.36 ± 1.32	0.26 ± 0.01	13.39 ± 4.80	0.06	0.01	0.21
	Surface-YSWM	28.22 ± 0.00	31.85 ± 0.00	0.47 ± 0.00	0.24 ± 0.00	0.68 ± 0.00			
	Bottom-YSWM	17.16 ± 0.00	32.28 ± 0.00	5.59 ± 0.00	0.30 ± 0.00	7.23 ± 0.00			
Autumn	YRDW	18.41 ± 0.05	25.96 ± 0.35	33.20 ± 1.63	0.29 ± 0.01	17.42 ± 0.36	0.07	0.01	0.12
	BSWM	19.32 ± 0.04	31.58 ± 0.01	6.19 ± 0.38	0.47 ± 0.04	9.85 ± 1.62			
	YSWM	17.41 ± 0.03	31.89 ± 0.00	6.56 ± 0.63	0.44 ± 0.02	6.43 ± 0.58			
Winter	BSCW	6.95 ± 0.01	29.26 ± 0.01	20.08 ± 0.29	0.24 ± 0.00	12.98 ± 0.25	0.07	0.01	0.22
	BSWM	7.54 ± 0.10	32.20 ± 0.09	8.32 ± 0.87	0.47 ± 0.06	11.36 ± 2.82			
	YSWM	10.14 ± 0.00	32.15 ± 0.00	5.18 ± 0.02	0.41 ± 0.05	8.34 ± 0.04			

ΔDIN, ΔDIP and ΔDSi were observed mainly in Central Bohai Sea in spring, most of the surface stations in summer, and nearshore regions in autumn and winter, corresponding to the higher Chl-*a* concentrations in these regions relative to other regions during the same period (Figures 2–5). Negative values of ΔDIN were observed in Bohai Bay from spring to autumn, but Chl-*a* concentrations in these areas were actually not low in summer and autumn, indicating external nutrient supplementation. One reason for this may be submarine groundwater discharge, which accounts for 80.8% of all DIN sources in the western Bohai Bay (Wang et al., 2020). Another reason may be associated with the high level of N-containing wastewater discharged by sewage discharge along Bohai Bay, which has exceeded 1500×10^6 tons per year (Liu et al., 2019). Significant negative ΔDIN values were also observed in Laizhou Bay in spring and summer, suggesting that there are other pathways of nutrient addition besides the Yellow River. This may be related to the submarine groundwater discharge, which is considered to derive significantly higher nutrient fluxes than the Yellow River (Zhang et al., 2016b). The apparent negative deviation of ΔDSi above the central shallow ridge in summer was caused by the dissolution of biogenic silica facilitated by the well vertical mixing of warm water in the region under the influence of mesoscale anticyclonic eddies (Loucaides et al., 2012; Liu et al., 2016; Wei et al., 2019). In addition, negative deviations in nutrients were observed at some stations in Central Bohai Sea in autumn and winter. Higher frequency and stronger strength of winds in the Bohai Sea during winter (Li et al., 2016) can cause significant sediment resuspension, thus contributing to higher local mineralization and nitrification rates (Ståhlberg et al., 2006; Xia et al., 2009; Niemistö et al., 2018).

Nutrients uptake ratios were estimated from model-derived assimilation of nutrients in euphotic zone, showing large seasonal differences (Figure 12). The average ΔDSi/ΔDIN uptake ratios were ca. 0.2 for spring, ca. 0.5 for summer, 0.8 for autumn and 1.1 for winter. The seasonal differences of ΔDSi/ΔDIN ratios were attributed to the difference of phytoplankton dominant species in different seasons. Studies have shown that diatoms prefer environments with low light and nutrient rich, while most dinoflagellates are heterotrophic or mixed trophic species, enabling them to adapt to waters with high light and low nutrient levels (Sun and Guo, 2011). As mentioned above, nutrients in autumn and winter were more abundant than those in late spring and summer in the Bohai Sea. Phytoplankton statistics results from the same cruise in autumn and winter showed a predominance of diatoms in terms of abundance, but high values of dinoflagellates (*Alexandrium* sp.) were also observed in autumn (Wang et al., 2022). The dominant diatoms in winter were *Paralia sulcate*, *Nitzschia* sp. and *Coscinodiscus* sp., which were usually characterized by highly silicification or relatively high Si/N ratio (Brzezinski, 1985; Mcquoid and Nordberg, 2003), with cells of *Nitzschia* sp. and *Coscinodiscus* sp. having Si/N ratios as high as 1.04-1.86 and 2.17, respectively (Brzezinski, 1985). Therefore, the average ΔDSi/ΔDIN ratio assimilated by phytoplankton was slightly higher than the canonical Redfield ratio in winter. While due to the influence of dinoflagellates, the average ΔDSi/ΔDIN ratio in autumn was slightly lower than the canonical Redfield ratio. A significant decrease in nutrient concentrations in spring was observed after siliceous organism bloom. The water bodies were in the presence of significant relatively Si limitation at the time of sampling. Correspondingly,

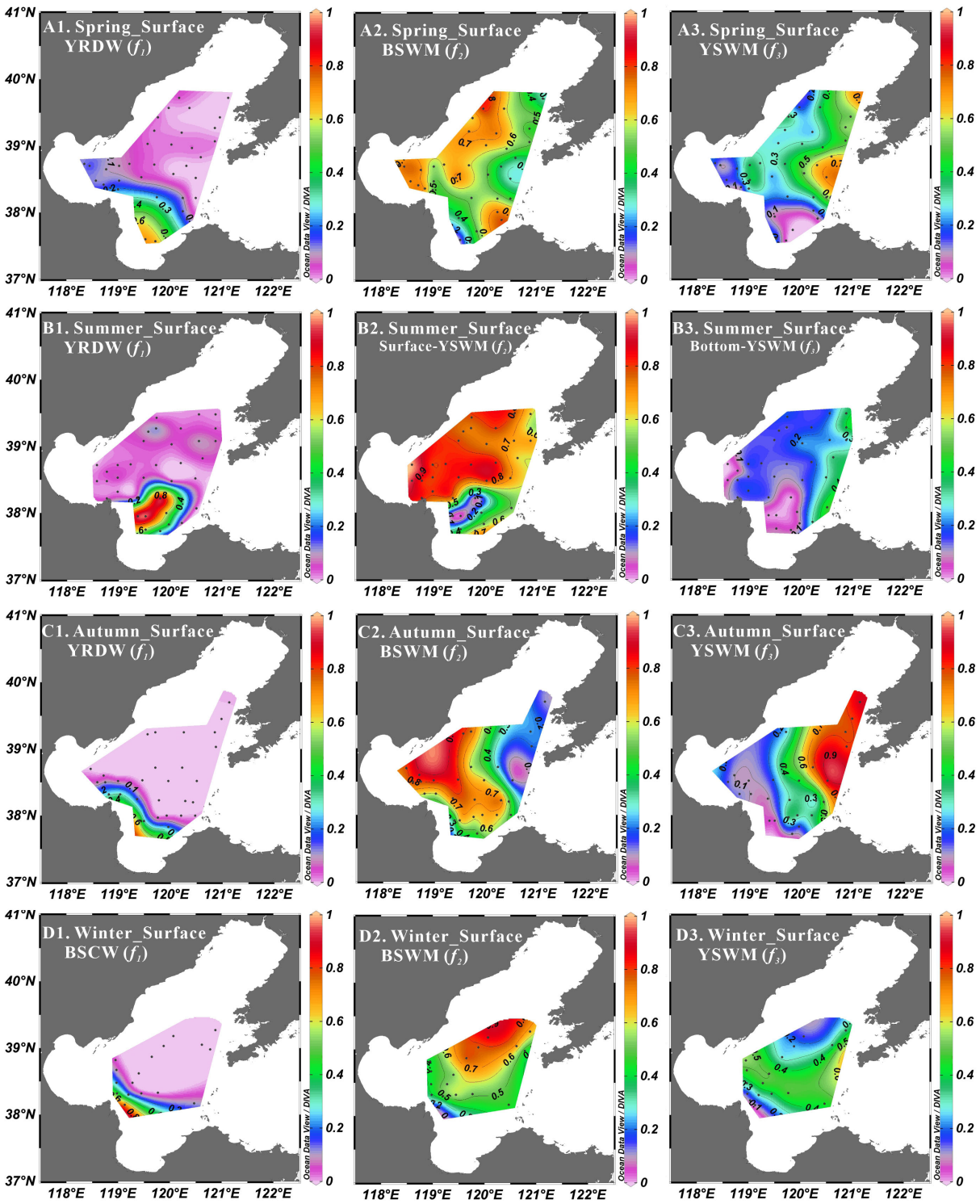

FIGURE 10
Three end-member composite fractions at surface layer in spring (A1, A2, A3), summer (B1, B2, B3), autumn (C1, C2, C3) and winter (D1, D2, D3).

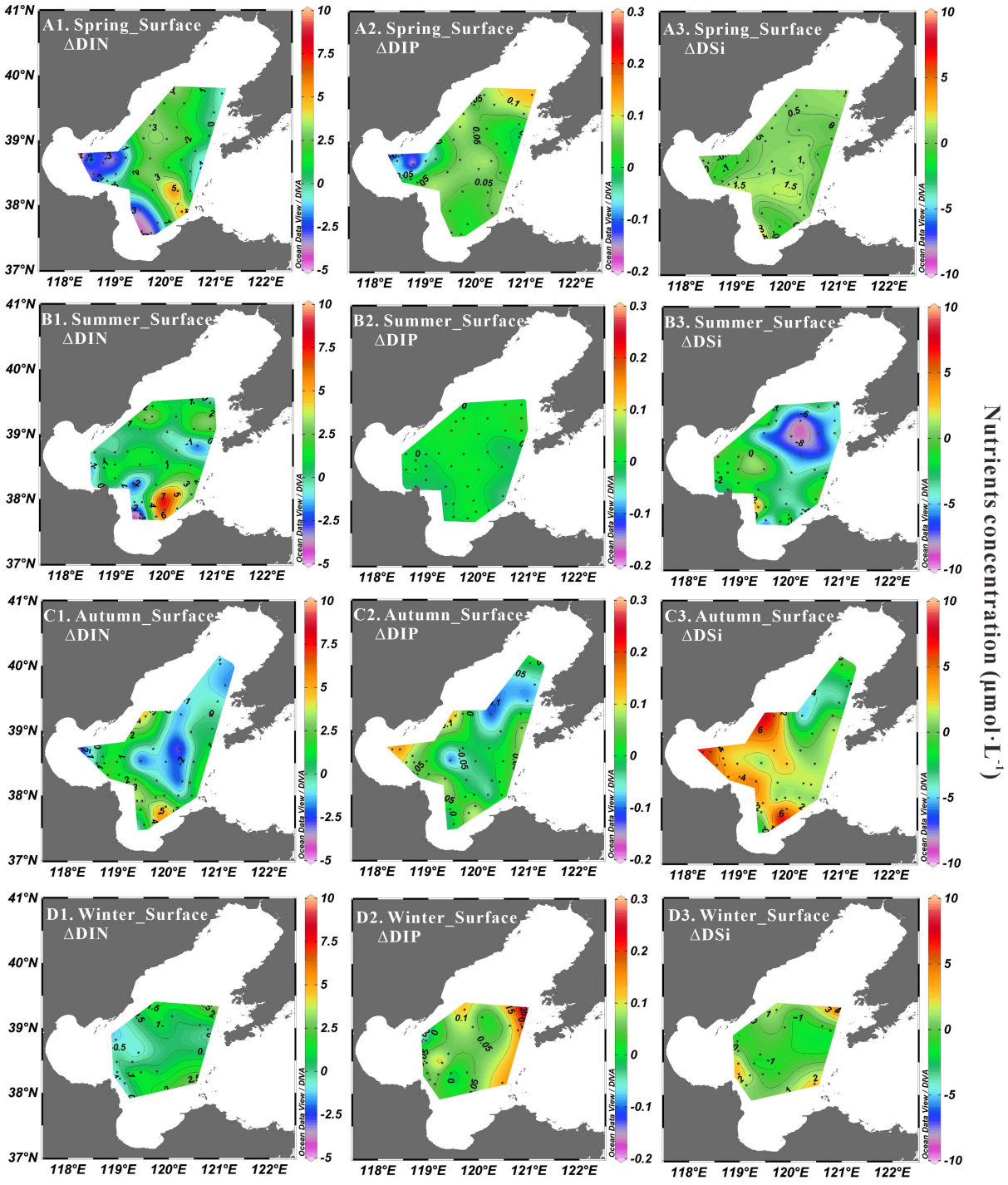

FIGURE 11
Nutrients deviation derived from the end-member mixing model at surface layer in spring (A1, A2, A3), summer (B1, B2, B3), autumn (C1, C2, C3) and winter (D1, D2, D3).

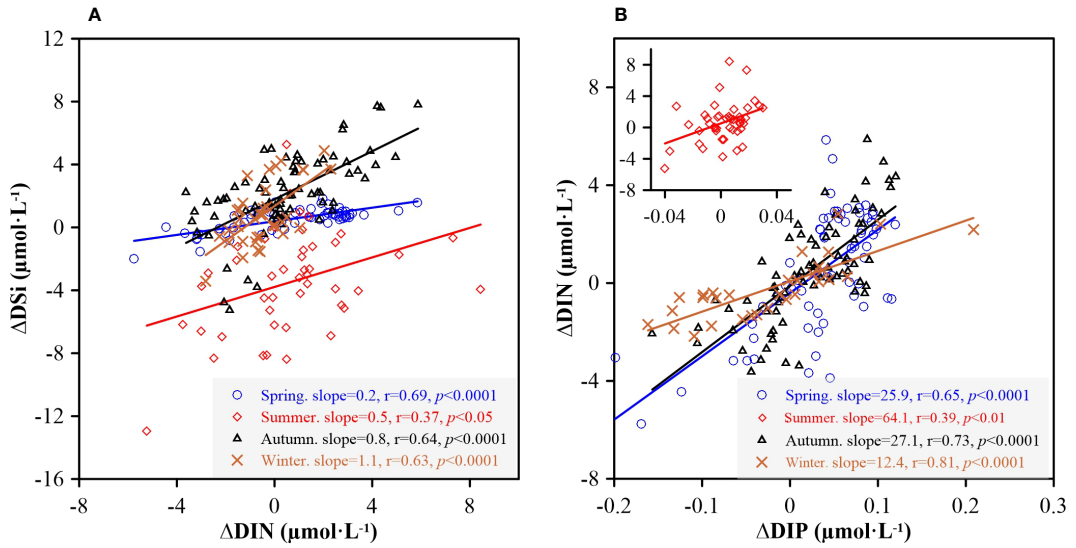

FIGURE 12
Relationship between ΔDSi *vs.* ΔDIN **(A)** and ΔDIN *vs.* ΔDIP **(B)** in euphotic zone.

the dominance of diatoms in the surface water of the Bohai Sea decreases significantly, and the average abundance of non-siliceous organisms such as cryptophytes, prasinophytes and dinoflagellates can account for ~49% of the total phytoplankton abundance (Zhang, 2016a). In summer, DIN and DIP concentrations remained significantly low, when the proportion of dinoflagellates increased to 52.7% and the proportion of diatoms decreased further to 46.4% (Hou et al., 2021). The abundance of these non-siliceous organisms well explained the low ΔDSi/ΔDIN ratio in spring and summer. Luan et al. (2018) summarized the long-term changes in phytoplankton communities in the Bohai Sea over the past 50 years and showed that the average dominance of diatoms was higher in winter than in autumn and significantly higher than in spring and summer, which was almost consistent with the seasonal differences in the ΔDSi/ΔDIN ratios in this study.

The average ΔDIN/ΔDIP uptake ratios were ca. 25.9 for spring, ca. 64.1 for summer, ca. 27.1 for autumn and ca. 12.4 for winter (Figure 12), which were within the range of phytoplankton uptake ratios (3-160) obtained from the *in-situ* incubation experiments in the Bohai Sea (Zou et al., 2001). Differences in ΔDIN/ΔDIP may be related to the fact that phytoplankton do not take up nutrients according to the canonical Redfield ratio (Klausmeier et al., 2004; Arrigo, 2005). Global patterns of marine plankton and organic matter elemental stoichiometry showed that plankton assemblages had different N/P ratios (Martiny et al., 2013). The average N/P ratio of phytoplankton community dominated by diatoms was ca. 13, comparable to the ΔDIN/ΔDIP ratio in our results in winter, where the absolutely dominant phytoplankton were diatoms (Yang et al., 2016; Wang et al., 2022). Studies have shown that the optimum N/P ratio for growth uptake of cryptophytes is higher than 16 (Schöllhorn and Granéli, 1997), which may explain the higher ΔDIN/ΔDIP ratio in spring. Lipsewers et al. (2020) investigated the effect of changes in dominance patterns on the stoichiometric ratio of phytoplankton in the Baltic Sea by applying community ordination (non-metric multidimensional scaling and generalized additive models). The results showed that the N/P ratios of phytoplankton ranged from 9 to 38 and increased with phytoplankton diversity. This may be a reasonable explanation for the higher ΔDIN/ΔDIP ratio in autumn, as Shannon-Wiener index in autumn has been shown to be the highest in all seasons in the Bohai Sea (Yang et al., 2016; Hou et al., 2021; Wang et al., 2022). The anomalously high ΔDIN/ΔDIP ratios for summer are explained in two aspects: Firstly, a stoichiometrically explicit model of phytoplankton physiology and resource competition showed that under the nitrogen limitation, the optimal strategy for phytoplankton produces a structural DIN/DIP ratio of 37.4 (Klausmeier et al., 2004), responding to the presence of significant relative nitrogen limitation in the Bohai Sea in summer in this study. Secondly, the rapid turnover cycle of phosphorus in the local environment may be another important reason for the low value of ΔDIP concentration and high ΔDIN/ΔDIP ratio in summer. The result from the $^{33}P/^{32}P$ ratios in dissolved and particulate matter in the East China Sea indicated a very short turnover rates of dissolved phosphorus (3–4 days) (Zhang Y. et al., 2004). This is significantly shorter than the

turnover rates (22-232 days) for nitrogen (Middelburg and Nieuwenhuize, 2000). Therefore, it is possible that the phosphorus in the local environment has experienced more times of absorption and remineralization than nitrogen in a short time. However, the limitations of the end-member mixing model cannot reflect these cycling processes.

4.3 Nutrient transport through turbulent entrainment in summer

As we discussed above, high Chl-*a* concentrations were a feature of the euphotic zone in summer, and the high primary production will rapidly assimilate nutrients in euphotic zone. Nutrient transport from the relatively nutrient-rich deep water across the thermocline to the euphotic zone is considered to be an important way for maintaining the continuous growth of phytoplankton in Central Bohai Sea during the stratification season. Based on equation (9), the entrainment velocity (W_{e1}) from the lower mixed layer to the upper mixed layer ranged from 1.0×10^{-6} m·s^{-1} to 48×10^{-6} m·s^{-1}, with an average of 10×10^{-6} m·s^{-1}. In this study, the concentrations of DIN, DIP and DSi in bottom water at the stratification station were 0.28-16.75 (average: 6.18 ± 4.19) μmol·L^{-1}, 0.17-0.37 (average: 0.28 ± 0.04) μmol·L^{-1} and 3.69-16.20 (average: 8.27 ± 2.92) μmol·L^{-1}, respectively. Therefore, the fluxes of nutrients entering the upper water through turbulent entrainment were estimated to be 0.14-52.59 (average: 6.04 ± 9.63) mmol·m^{-2}·d^{-1} for DIN, 0.03-0.90 (average: 0.22 ± 0.19) mmol·m^{-2}·d^{-1} for DIP and 0.49-26.26 (average: 6.97 ± 6.61) mmol·m^{-2}·d^{-1} for DSi, respectively. Plots of the relationship between nutrient fluxes *via* turbulent entrainment and Chl-*a* concentrations at surface layer were shown in Supplementary Figure 3. The results showed nutrient fluxes had a good positive correlation with Chl-*a* concentration ($p< 0.01$).

Compared to nearshore areas, Central Bohai Sea was relatively less affected by riverine inputs, while atmospheric deposition was generally considered to be another important nutrient source for Central Bohai Sea (Shou et al., 2018; Zheng et al., 2020). Based on the average dry deposition rate and nutrients in atmospheric aerosols from August to September 2017 (Qi et al., 2020), the average dry deposition flux of inorganic nitrogen (the sum of NO_3^- and NH_4^+) and phosphorus in the Bohai Sea in summer were estimated to be 0.63 mmol·m^{-2}·d^{-1} for nitrogen and 0.0005 mmol·m^{-2}·d^{-1} for phosphorus, respectively. Wet deposition in the Bohai Sea was estimated as 54–68% of total deposition (Liu et al., 2003; Zhang et al., 2008; Zhao Y. et al., 2017). Therefore, the total dry and wet deposition flux of nutrients was estimated to be 1.36-1.96 mmol·m^{-2}·d^{-1} for nitrogen and 0.001-0.0015 mmol·m^{-2}·d^{-1} for phosphorus, respectively. Data for silicon from atmospheric deposition in summer were scarce, but the average flux of silicon was ca. 0.007 mmol·m^{-2}·d^{-1} as estimated by Zhang J. et al. (2004). Thus, the average nitrogen flux from atmospheric deposition was of the same order of magnitude as the average nitrogen flux through turbulent entrainment, with the latter higher than the former. However, the average phosphorus or silicon flux from atmospheric deposition was 3 or 4 orders of magnitude lower than the average phosphorus or silicon flux through turbulent entrainment, respectively. Overall, compared to atmospheric deposition, nutrients *via* turbulent entrainment were more important for sustaining phytoplankton growth in euphotic zone during the stratification period from our study, especially for phosphorus and silicon.

Based on Redfield ratios (C:N = 106:16), the primary production *via* turbulent entrainment and atmospheric deposition of nitrogen in Central Bohai Sea in summer was estimated to be 560.21 ± 893.18 mg C·m^{-2}·d^{-1} and 126.14-181.79 mg C·m^{-2}·d^{-1}, respectively. While the primary production in the entire Bohai Sea in August was estimated to be ~1600 mg C·m^{-2}·d^{-1} (Tan et al., 2011), so the primary production in Central Bohai Sea in summer was estimated to be ~1280 mg C·m^{-2}·d^{-1} based on the fact that the average Chl-*a* concentration in Central Bohai Sea was 80% of that in the entire study area in this study. Thus, nitrogen *via* turbulent entrainment and atmospheric deposition can contribute ~44% and 10%-14% of the primary productivity, respectively.

5 Conclusion

The concentration of dissolved inorganic nutrients was mainly characterized by depletion throughout the water column in spring and in the euphotic zone in summer, and conversely by accumulation in the bottom water in summer, and in the water column in autumn and winter. The dominant component of DIN was NH_4^+ in summer and NO_3^- in other seasons, while DON was the main form of TDN in all seasons. Compared to the average percentage of DIP in TDP,the average percentage of DOP in TDP was significantly higher in spring and comparable in otherseasons. The nutrient limitation for phytoplankton growth showed seasonal and regional variations, with relative phosphorus limitation in Laizhou Bay and the Yellow River Estuary in all seasons, relative silicon limitation in the most area in spring and relative nitrogen limitation in most offshore area in summer. Our results suggest that nutrient uptake rates varied between seasons and do not exactly follow the canonical Redfield ratio under the influence of the different phytoplankton composition and phosphorus turnover rate. Turbulent entrainment is an important nutrient source pathway for the euphotic zone of Central Bohai Sea in

summer. The average nitrogen fluxes from turbulent entrainment were in the same order of magnitude as that from atmospheric deposition, but the average phosphorus or silicon fluxes from the former are 3 or 4 orders of magnitude higher than the latter, respectively.

Data availability statement

The raw data supporting the conclusions of this article will be made available by the authors, without undue reservation.

Author contributions

WL and SL: conception and design of study. SL: financial support. WL: drafting the manuscript. SL: revising the manuscript. WL, SL, and LZ: methodology. WL, YW, MW: sample determination. YW, MW, CCL, XZ, N W, LW, DZ, YM, and CL: Investigation. All authors contributed to the article and approved the submitted version.

Funding

This study was funded by the National Natural Science Foundation of China-Shandong Joint Foundation (NSFC: U1806211), and the National Key Research and Development Program of China (2016YFA0600902). This study is a contribution to the IMBeR/FEC–CMWG Program.

Acknowlegments

WL would like to thank Dr. Tian Shichao for his help in the mixing model.

Conflict of interest

The authors declare that the research was conducted in the absence of any commercial or financial relationships that could be construed as a potential conflict of interest.

Publisher's note

Supplementary material

The Supplementary Material for this article can be found online at: https://www.frontiersin.org/articles/10.3389/fmars.2022.1025502/full#supplementary-material

References

Arrigo, K. R. (2005). Marine microorganisms and global nutrient cycles. *Nature* 437, 349–355. doi: 10.1038/nature04265

Barmawidjaja, D. M., van der Zwaan, G. J., Jorissen, F. J., and Puskaric, S. (1995). 150 years of eutrophication in the northern Adriatic Sea: evidence from a benthic foraminiferal record. *Mar. Geol.* 122, 367–384. doi: 10.1016/0025-3227(94)00121-Z

Bristow, L. A., Mohr, W., Ahmerkamp, S., and Kuypers, M. M. (2017). Nutrients that limit growth in the ocean. *Curr. Biol.* 27, R474–R478. doi: 10.1016/j.cub.2017.03.030

Brzezinski, M. A. (1985). The Si: C: N ratio of marine diatoms: interspecific variability and the effect of some environmental variables. *J. Phycol.* 21, 347–357. doi: 10.1111/j.0022-3646.1985.00347.x

Cui, Y., Chen, B. J., and Chen, J. F. (2005). Evaluation on self-pollution of marine culture in the yellow Sea and bohai Sea. *Chin. J. Appl. Ecol.* 16, 180–185. doi: 10.13287/j.1001-9332.2005.0412

Ding, X., Guo, X., Zhang, C., Yao, X., Liu, S., Shi, J., et al. (2020). Water conservancy project on the yellow river modifies the seasonal variation of chlorophyll-a in the bohai Sea. *Chemosphere* 254, 126846. doi: 10.1016/j.chemosphere.2020.126846

Dong, Z., Liu, D., and Keesing, J. K. (2010). Jellyfish blooms in China: dominant species, causes and consequences. *Mar. pollut. Bull.* 60, 954–963. doi: 10.1016/j.marpolbul.2010.04.022

Fang, Y., Fang, G. H., and Zhang, Q. H. (2000). Numerical simulation and dynamic study of the wintertime circulation of the bohai Sea. *Chin. J. Oceanol. Limnol.* 18, 1–9. doi: 10.1007/BF02842535-

Fitzsimons, M. F., Probert, I., Gaillard, F., and Rees, A. P. (2020). Dissolved organic phosphorus uptake by marine phytoplankton is enhanced by the presence of dissolved organic nitrogen. *J. Exp. Mar. Biol. Ecol.* 530, 151434. doi: 10.1016/j.jembe.2020.151434

Fu, Y., Xu, S., and Liu, J. (2016). Temporal-spatial variations and developing trends of chlorophyll-a in the bohai Sea, China. *Estuar. Coast. Shelf Sci.* 173, 49–56. doi: 10.1016/j.ecss.2016.02.016

Glover, D. M., and Brewer, P. G. (1988). Estimates of wintertime mixed layer nutrient concentrations in the north Atlantic. *Deep Sea Res. Part A* 35, 1525–1546. doi: 10.1016/0198-0149(88)90101-X

Grasshoff, K., Kremling, K., and Ehrhardt, M. (1999). *Methods of seawater analysis. 3rd edition* (Weinheim: WILEY–VCH Verlag GmbH), 203–223.

Han, A., Dai, M., Kao, S. J., Gan, J., Li, Q., Wang, L., et al. (2012). Nutrient dynamics and biological consumption in a large continental shelf system under the influence of both a river plume and coastal upwelling. *Limnol. Oceanogr.* 57, 486–502. doi: 10.4319/lo.2012.57.2.0486

Han, H., Song, W., Wang, Z., Ding, D., Yuan, C., Zhang, X., et al. (2019). Distribution of green algae micro-propagules and their function in the formation of the green tides in the coast of qinhuangdao, the bohai Sea, China. *Acta Oceanol. Sin.* 38, 72–77. doi: 10.1007/s13131-018-1278-1

Holmes, R. M., Aminot, A., Kérouel, R., Hooker, B. A., and Peterson, B. J. (1999). A simple and precise method for measuring ammonium in marine and freshwater ecosystems. *Can. J. Fish. Aquat. Sci.* 56, 1801–1808. doi: 10.1139/cjfas-56-10-1801

Hou, T., Wang, S., Chen, H., Zhuang, Y., Liu, G., and Wang, N. (2021). Characterization and comparison of phytoplankton community structure in the

bohai Sea and yellow Sea in summer 2013. *Mar. Environ. Sci.* 40, 591–600. doi: 10.13634/j.cnki.mes.2021.04.016

Huang, R., Chen, J., Wang, L., and Lin, Z. (2012). Characteristics, processes, and causes of the spatio-temporal variabilities of the East Asian monsoon system. *Adv. Atmos. Sci.* 29, 910–942. doi: 10.1007/s00376-012-2015-x

Ichiro, I., Mineo, Y., and Yutaka, H. (2006). Eutrophication and occurrences of harmful algal blooms in the seto inland Sea, Japan. *Plankton Benthos Res.* 1, 71–84. doi: 10.3800/pbr.1.71

Kara, A. B., Rochford, P. A., and Hurlburt, H. E. (2000). An optimal definition for ocean mixed layer depth. *J. Geophys. Res.* 105, 16803–16821. doi: 10.1029/2000JC900072

Kemp, W. M., Boynton, W. R., Adolf, J. E., Boesch, D. F., Boicourt, W. C., Brush, G., et al. (2005). Eutrophication of Chesapeake bay: historical trends and ecological interactions. *Mar. Ecol. Prog. Ser.* 303, 1–29. doi: 10.3354/meps303001

Klausmeier, C. A., Litchman, E., Daufresne, T., and Levin, S. A. (2004). Optimal nitrogen-to-phosphorus stoichiometry of phytoplankton. *Nature* 429, 171–174. doi: 10.1038/nature02454

Li, G., Liang, Q., and Li, B. (2003). Remote sensing inversion of the euphotic layer depth in the East China Sea and its influence mechanism. *Prog. Nat. Sci.* 13, 90–94. doi: 10.3321/j.issn:1002-008X.2003.01.017

Lin, L., Liu, D., Guo, X., Luo, C., and Cheng, Y. (2020). Tidal effect on water export rate in the eastern shelf seas of China. *J. Geophys. Res.* 125, e2019JC015863. doi: 10.1029/2019JC015863

Lin, X., Xie, S. P., Chen, X., and Xu, L. (2006). A well-mixed warm water column in the central bohai Sea in summer: Effects of tidal and surface wave mixing. *J. Geophys. Res.* 111, C11. doi: 10.1029/2006JC003504

Lipsewers, T., Klais, R., Camarena-Gómez, M. T., and Spilling, K. (2020). Effects of different plankton communities and spring bloom phases on seston c: N: P: Si: chl a ratios in the Baltic Sea. *Mar. Ecol. Prog. Ser.* 644, 15–31. doi: 10.3354/meps13361

Liu, S. M. (2015). Response of nutrient transports to water–sediment regulation events in the huanghe basin and its impact on the biogeochemistry of the bohai. *J. Mar. Syst.* 141, 59–70. doi: 10.1016/j.jmarsys.2014.08.008

Liu, S. M., Altabet, M. A., Zhao, L., Larkum, J., Song, G. D., Zhang, G. L., et al. (2017). Tracing nitrogen biogeochemistry during the beginning of a spring phytoplankton bloom in the yellow Sea using coupled nitrate nitrogen and oxygen isotope ratios. *J. Geophys. Res.* 122, 2490–2508. doi: 10.1002/2016JG003752

Liu, J., Du, J., and Yi, L. (2017). Ra Tracer-based study of submarine groundwater discharge and associated nutrient fluxes into the bohai Sea, China: A highly human-affected marginal sea. *J. Geophys. Res.* 122, 8646–8660. doi: 10.1002/2017JC013095

Liu, S. M., Hong, G. H., Zhang, J., Ye, X. W., and Jiang, X. L. (2009). Nutrient budgets for large Chinese estuaries. *Biogeosciences* 6, 2245–2263. doi: 10.5194/bg-6-2245-2009

Liu, X., Liu, D., Wang, Y., Shi, Y., Wang, Y., and Sun, X. (2019). Temporal and spatial variations and impact factors of nutrients in bohai bay, China. *Mar. pollut. Bull.* 140, 549–562. doi: 10.1016/j.marpolbul.2019.02.011

Liu, S. M., Li, L. W., and Zhang, Z. (2011). Inventory of nutrients in the bohai. *Cont. Shelf Res.* 31 (16), 1790–1797. doi: 10.1016/j.csr.2011.08.004

Liu, S. M., Li, L. W., Zhang, G. L., Liu, Z., Yu, Z., and Ren, J. L. (2012). Impacts of human activities on nutrient transports in the huanghe (Yellow river) estuary. *J. Hydrol.* 430, 103–110. doi: 10.1016/j.jhydrol.2012.02.005

Liu, J., Zang, J., Bouwman, L., Liu, S., Yu, Z., and Ran, X. (2016). Distribution and budget of dissolved and biogenic silica in the bohai Sea and yellow Sea. *Biogeochemistry* 130, 85–101. doi: 10.1007/s10533-016-0244-2

Liu, S. M., Zhang, J., Gao, H. W., and Liu, Z. (2008). Historic changes in flux of matter and nutrient budgets in the bohai Sea. *Acta Oceanol. Sin.* 27, 81–97. doi: 10.1145/1360612.1360695

Liu, S. M., Zhang, J., and Jiang, W. S. (2003). Pore water nutrient regeneration in shallow coastal bohai Sea, China. *J. Oceanogr.* 59, 377–385. doi: 10.1023/A:1025576212927

Li, D., von Storch, H., and Geyer, B. (2016). High-resolution wind hindcast over the bohai Sea and the yellow Sea in East Asia: Evaluation and wind climatology analysis. *J. Geophys. Res.* 121, 111–129. doi: 10.1002/2015JD024177

Li, Y., Wolanski, E., and Zhang, H. (2015). What processes control the net currents through shallow straits? a review with application to the bohai strait, China. *Estuar. Coast. Shelf Sci.* 158, 1–11. doi: 10.1016/j.ecss.2015.03.013

Loucaides, S., Van Cappellen, P., Roubeix, V., Moriceau, B., and Ragueneau, O. (2012). Controls on the recycling and preservation of biogenic silica from biomineralization to burial. *Silicon* 4, 7–22. doi: 10.1007/s12633-011-9092-9

Luan, Q. S., Kang, Y. D., and Wang, J. (2018). Long-term changes on phytoplankton community in the bohai Sea, (1959~2015). *Prog. Fish. Sci.* 39, 09–18. doi: 10.19663/j.issn2095-9869.20180329001

Luo, Y. M. (2020). *Evolution of environment and ecosystem in the bohai Sea and coast* (Beijing: Science Press).

Martiny, A. C., Pham, C. T., Primeau, F. W., Vrugt, J. A., Moore, J. K., Levin, S. A., et al. (2013). Strong latitudinal patterns in the elemental ratios of marine plankton and organic matter. *Nat. Geosci.* 6, 279–283. doi: 10.1038/NGEO1757

Mcquoid, M. R., and Nordberg, K. (2003). The diatom paralia sulcata as an environmental indicator species in coastal sediments. *Estuar. Coast. Shelf Sci.* 56, 339–354. doi: 10.1016/S0272-7714(02)00187-7

Middelburg, J. J., and Nieuwenhuize, J. (2000). Nitrogen uptake by heterotrophic bacteria and phytoplankton in the nitrate-rich Thames estuary. *Mar. Ecol. Prog. Ser.* 203, 13–21. doi: 10.3354/meps203013

Niemistö, J., Kononets, M., Ekeroth, N., Tallberg, P., Tengberg, A., and Hall, P. O. (2018). Benthic fluxes of oxygen and inorganic nutrients in the archipelago of gulf of Finland, Baltic Sea–effects of sediment resuspension measured *in situ*. *J. Sea Res.* 135, 95–106. doi: 10.1016/j.seares.2018.02.006

Ning, X., Lin, C., Su, J., Liu, C., Hao, Q., Le, F., et al. (2010). Long-term environmental changes and the responses of the ecosystems in the bohai Sea during 1960–1996. *Deep Sea Res. Part II* 57, 1079–1091. doi: 10.1016/j.dsr2.2010.02.010

Pan, G., Krom, M. D., Zhang, M., Zhang, X., Wang, L., Dai, L., et al. (2013). Impact of suspended inorganic particles on phosphorus cycling in the yellow river (China). *Environ. Sci. Technol.* 47, 9685–9692. doi: 10.1021/es4005619

Parsons, T. R., Maita, Y., and Lalli, C. M. (1984). *A manual of chemical and biological methods for seawater analysis* (Oxford: Pergamon Press).

Qi, J., Yu, Y., Yao, X., Gang, Y., and Gao, H. (2020). Dry deposition fluxes of inorganic nitrogen and phosphorus in atmospheric aerosols over the marginal seas and Northwest pacific. *Atmos. Res.* 245, 105076. doi: 10.1016/j.atmosres.2020.105076

Ren, J., Lei, X., Zhang, Y., Wang, M., and Xiang, L. (2017). Sunshine duration variability in haihe river basin, China, during 1966–2015. *Water* 9, 770. doi: 10.3390/w9100770

Ren, Y., Zhao, Y., and Zhang, B. (1990). Heat balance at the bohai Sea, huanghai Sea and East China Sea surface II. characteristics of the seasonal variation. *Mar. Sci.* 5, 18–24.

Riegman, R., Noordeloos, A. A. M., and Cadée, G. C. (1992). Phaeocystis blooms and eutrophication of the continental coastal zones of the north Sea. *Mar. Biol.* 112, 479–484. doi: 10.1007/BF00356293

RockstrÖm, J., Steffen, W., and Noone, K. (2009). A safe operating space for humanity. *Nature* 461, 472–475. doi: 10.1038/461472a

Schöllhorn, E., and Granéli, W. (1997). The importance of increasing N/P ratios for phytoplankton biomass and species composition in an oligotrophic lake. *Internationale Vereinigung für theoretische und angewandte Limnologie: Verhandlungen* 26, 615–620. doi: 10.1080/03680770.1995.11900791

Shi, X., Qi, M., Tang, H., and Han, X. (2015). Spatial and temporal nutrient variations in the yellow Sea and their effects on ulva prolifera blooms. *Estuar. Coast. Shelf Sci.* 163, 36–43. doi: 10.1016/j.ecss.2015.02.007

Shou, W., Zong, H., Ding, P., and Hou, L. (2018). A modelling approach to assess the effects of atmospheric nitrogen deposition on the marine ecosystem in the bohai Sea, China. *Estuar. Coast. Shelf Sci.* 208, 36–48. doi: 10.1016/j.ecss.2018.04.025

Song, N. Q., Wang, N., Lu, Y., and Zhang, J. R. (2016). Temporal and spatial characteristics of harmful algal blooms in the bohai Sea during 1952–2014. *Cont. Shelf Res.* 122, 77–84. doi: 10.1016/j.csr.2016.04.006

Song, G., Zhao, L., Chai, F., Liu, F., Li, M., and Xie, H. (2020). Summertime oxygen depletion and acidification in bohai Sea, China. *Front. Mar. Sci.* 7. doi: 10.3389/fmars.2020.00252

Ståhlberg, C., Bastviken, D., Svensson, B. H., and Rahm, L. (2006). Mineralisation of organic matter in coastal sediments at different frequency and duration of resuspension. *Estuar. Coast. Shelf Sci.* 70, 317–325. doi: 10.1016/j.ecss.2006.06.022

Steffen, W., Richardson, K., Rockström, J., Cornell, S. E., Fetzer, I., Bennett, E. M., et al. (2015). Planetary boundaries: Guiding human development on a changing planet. *Science* 347, 1259855. doi: 10.1126/science.aaa9629

Stigebrandt, A. (1981). "Cross thermocline flow on continental shelves and the locations of shelf fronts," in *Elsevier oceanography series*, ed. J. C. J. Nihoul (Amsterdam: Elsevier) 32, 51–65. doi: 10.1016/S0422-9894(08)70403-3

Sun, J., and Guo, S. J. (2011). Dinoflagellate heterotrophy. *Acta Ecol. Sin.* 31, 6270–6286.

Sun, J., Liu, D., and Qian, S. (2001). Preliminary study on seasonal succession and development pathway of phytoplankton community in the bohai Sea. *Acta Oceanol. Sin.* 20, 251–260.

Tan, S. C., Shi, G. Y., Shi, J. H., Gao, H. W., and Yao, X. (2011). Correlation of Asian dust with chlorophyll and primary productivity in the coastal seas of China

during the period from 1998 to 2008. *J. Geophys. Res.* 116, G02029. doi: 10.1029/2010JG001456

Taylor, J. R. (1997). *An introduction to error analysis: The study of uncertainties in physical measurements*, *2nd* ed. Sausalito: University Science Books.

Turner, R. E., Rabalais, N. N., and Zhang, Z. N. (1990). Phytoplankton biomass, production and growth limitations on the huanghe (Yellow river) continental shelf. *Cont. Shelf Res.* 10, 545–571. doi: 10.1016/0278-4343(90)90081-V

Tyrrell, T. (1999). The relative influences of nitrogen and phosphorus on oceanic primary production. *Nature* 400, 525–531. doi: 10.1038/22941

Voss, M., Dippner, J. W., Humborg, C., Hürdler, J., Korth, F., Neumann, T., et al. (2011). History and scenarios of future development of Baltic Sea eutrophication. *Estuar. Coast. Shelf Sci.* 92, 307–322. doi: 10.1016/j.ecss.2010.12.037

Wang, J., Beusen, A. H., Liu, X., and Bouwman, A. F. (2019b). Aquaculture production is a large, spatially concentrated source of nutrients in Chinese freshwater and coastal seas. *Environ. Sci. Technol.* 54, 1464–1474. doi: 10.1021/acs.est.9b03340

Wang, K., Chen, J., Jin, H., Li, H., Gao, S., Xu, J., et al. (2014). Summer nutrient dynamics and biological carbon uptake rate in the changjiang river plume inferred using a three end-member mixing model. *Cont. Shelf Res.* 91, 192–200. doi: 10.1016/j.csr.2014.09.013

Wang, X., Cui, Z., Guo, Q., Han, X., and Wang, J. (2009). Distribution of nutrients and eutrophication assessment in the bohai Sea of China. *Chin. J. Oceanol. Limnol.* 27, 177–183. doi: 10.1007/s00343-009-0177-x

Wang, Q., Li, H., Zhang, Y., Wang, X., Xiao, K., Zhang, X., et al. (2020). Submarine groundwater discharge and its implication for nutrient budgets in the western bohai bay, China. *J. Environ. Radioact.* 212, 106132. doi: 10.1016/j.jenvrad.2019.106132

Wang, B., Xin, M., Wei, Q., and Xie, L. (2018). A historical overview of coastal eutrophication in the China seas. *Mar. pollut. Bull.* 136, 394–400. doi: 10.1016/j.marpolbul.2018.09.044

Wang, X., Yang, S., and Zhang, Q. (2022). Coupling effect of phytoplankton community structure and environmental factors in the bohai Sea of China. *Mar. pollut. Bull.* 179, 113707. doi: 10.1016/j.marpolbul.2022.113707

Wang, J., Yu, Z., Wei, Q., and Yao, Q. (2019a). Long-term nutrient variations in the bohai Sea over the past 40 years. *J. Geophys. Res.* 124, 703–722. doi: 10.1029/2018JC014765

Wei, H., Wang, L., Lin, Y. A., and Chung, C. S. (2002). Nutrient transport across the thermocline in the central yellow Sea. *Adv. Mar. Sci.* 20, 15–20. doi: 10.3969/j.issn.1671-6647.2002.03.003

Wei, Q., Wang, B., Yao, Q., Xue, L., Sun, J., Xin, M., et al. (2019). Spatiotemporal variations in the summer hypoxia in the bohai Sea (China) and controlling mechanisms. *Mar. pollut. Bull.* 138, 125–134. doi: 10.1016/j.marpolbul.2018.11.041

Wu, N., Liu, S. M., Zhang, G. L., and Zhang, H. M. (2021). Anthropogenic impacts on nutrient variability in the lower yellow river. *Sci. Total Environ.* 755, 142488. doi: 10.1016/j.scitotenv.2020.142488

Wu, L., Wang, J., Gao, S., Zheng, X., and Huang, R. (2017). An analysis of dynamical factors influencing 2013 giant jellyfish bloom near qinhuangdao in the bohai Sea, China. *Estuar. Coast. Shelf Sci.* 185, 141–151. doi: 10.1016/j.ecss.2016.12.010

Xia, X., Yang, Z., and Zhang, X. (2009). Effect of suspended-sediment concentration on nitrification in river water: importance of suspended sediment–water interface. *Environ. Sci. Technol.* 43, 3681–3687. doi: 10.1021/es8036675

Xin, M., Wang, B., Xie, L., Sun, X., Wei, Q., Liang, S., et al. (2019). Long-term changes in nutrient regimes and their ecological effects in the bohai Sea, China. *Mar. pollut. Bull.* 146, 562–573. doi: 10.1016/j.marpolbul.2019.07.011

Xu, P., Yang, W., Zhao, L., Wei, H., and Nie, H. (2020). Observations of turbulent mixing in the bohai Sea during weakly stratified period. *Acta Oceanol. Sin.* 42, 1–9. doi: 10.3969/j.issn.0253–4193.2020.03.001

Yang, Y., Sun, J., Guan, X., Zhai, W., and Guo, S. (2016). Seasonal variation of netz-phytoplankton community in bohai Sea. *Mar. Sci. Bull.* 5, 121–131. doi: 10.11840/j.issn.1001-6392.2016.02.001

Yang, D., Zhou, D., and Zhang, Y. (1991). The effect of tidal–mixing across thermocline in coastal sea. *Acta Oceanol. Sin.* 13, 295—304.

Yunev, O. A., Carstensen, J., Moncheva, S., Khaliulin, A., Ærtebjerg, G., and Nixon, S. (2007). Nutrient and phytoplankton trends on the western black Sea shelf in response to cultural eutrophication and climate changes. *Estuar. Coast. Shelf Sci.* 74, 63–76. doi: 10.1016/j.ecss.2007.03.030

Zhai, F., Wu, W., Gu, Y., Li, P., Song, X., Liu, P., et al. (2021). Interannual-decadal variation in satellite-derived surface chlorophyll-a concentration in the bohai Sea over the past 16 years. *J. Mar. Syst.* 215, 103496. doi: 10.1016/j.jmarsys.2020.103496

Zhai, W. D., Zhao, H. D., Su, J. L., Liu, P. F., Li, Y. W., and Zheng, N. (2019). Emergence of summertime hypoxia and concurrent carbonate mineral suppression in the central bohai Sea, China. *J. Geophys. Res.* 124, 2768–2785. doi: 10.1029/2019JG005120

Zhai, W., Zhao, H., Zheng, N., and Xu, Y. (2012). Coastal acidification in summer bottom oxygen-depleted waters in northwestern-northern bohai Sea from June to august in 2011. *Chin. Sci. Bull.* 57, 1062–1068. doi: 10.1007/s11434-011-4949-2

Zhang, Y. (2016a). Spatial correlation and seasonal variation of phytoplankton and environmental factors in the central bohai Sea. [Master's thesis]. [Yantai (CN): Yantai Institute of Coastal Zone Research, Chinese Academy of Sciences].

Zhang, Z., Cao, Y., and Zhao, W. (2011). Wind characteristics and land-sea wind speed comparison in the bohai bay. *Mar. Forecasts* 28, 33–39. doi: 10.3969/j.issn.1003-0239.2011.06.006

Zhang, G., Liang, S., Shi, X., and Han, X. (2015). Dissolved organic nitrogen bioavailability indicated by amino acids during a diatom to dinoflagellate bloom succession in the changjiang river estuary and its adjacent shelf. *Mar. Chem.* 176, 83–95. doi: 10.1016/j.marchem.2015.08.001

Zhang, Y., Liu, X. J., Fangmeier, A., Goulding, K. T. W., and Zhang, F. S. (2008). Nitrogen inputs and isotopes in precipitation in the north China plain. *Atmos. Environ.* 42, 1436–1448. doi: 10.1016/j.atmosenv.2007.11.002

Zhang, Y., Li, H., Wang, X., Zheng, C., Wang, C., Xiao, K., et al. (2016b). Estimation of submarine groundwater discharge and associated nutrient fluxes in eastern laizhou bay, China using 222Rn. *J. Hydrol.* 533, 103–113. doi: 10.1016/j.jhydrol.2015.11.027

Zhang, H., Qiu, Z., Sun, D., Wang, S., and He, Y. (2017). Seasonal and interannual variability of satellite-derived chlorophyll-a, (2000–2012) in the bohai Sea, China. *Remote Sens.* 9, 582. doi: 10.3390/rs9060582

Zhang, Q. C., Qiu, L. M., Yu, R. C., Kong, F. Z., Wang, Y. F., Yan, T., et al. (2012). Emergence of brown tides caused by aureococcus anophagefferens hargraves et sieburth in China. *Harmful Algae* 19, 117–124. doi: 10.1016/j.hal.2012.06.007

Zhang, S. F., Yuan, C. J., Chen, Y., Lin, L., and Wang, D. Z. (2019). Transcriptomic response to changing ambient phosphorus in the marine dinoflagellate prorocentrum donghaiense. *Sci. Total Environ.* 692, 1037–1047. doi: 10.1016/j.scitotenv.2019.07.291

Zhang, J., Yu, Z. G., Raabe, T., Liu, S. M., Starke, A., Zou, L., et al. (2004). Dynamics of inorganic nutrient species in the bohai seawaters. *J. Mar. Syst.* 44, 189–212. doi: 10.1016/j.jmarsys.2003.09.010

Zhang, Y., Zhu, L., Zeng, X., and Lin, Y. (2004). The biogeochemical cycling of phosphorus in the upper ocean of the East China Sea. *Estuar. Coast. Shelf Sci.* 60, 369–379. doi: 10.1016/j.ecss.2004.02.001

Zhao, H. D., Kao, S. J., Zhai, W. D., Zang, K. P., Zheng, N., Xu, X. M., et al. (2017). Effects of stratification, organic matter remineralization and bathymetry on summertime oxygen distribution in the bohai Sea, China. *Cont. Shelf Res.* 134, 15–25. doi: 10.1016/j.csr.2016.12.004

Zhao, L., and Wei, H. (2001). Annual cycle of the vertical eddy viscosity in the bohai Sea. *J. Ocean Univ. Qingdao* 31, 313–318. doi: 10.16441/j.cnki.hdxb.2001.03.003

Zhao, Y., Zhang, L., Chen, Y., Liu, X., Xu, W., Pan, Y., et al. (2017). Atmospheric nitrogen deposition to China: A model analysis on nitrogen budget and critical load exceedance. *Atmos. Environ.* 153, 32–40. doi: 10.1016/j.atmosenv.2017.01.018

Zheng, L. W., Zhai, W. D., Wang, L. F., and Huang, T. (2020). Improving the understanding of central bohai Sea eutrophication based on wintertime dissolved inorganic nutrient budgets: Roles of north yellow Sea water intrusion and atmospheric nitrogen deposition. *Environ. pollut.* 267, 115626. doi: 10.1016/j.envpol.2020.115626

Zhou, F., Huang, D. J., and Su, J. L. (2009). Numerical simulation of the dual-core structure of the bohai Sea cold bottom water in summer. *Chin. Sci. Bull.* 54, 4520–4528. doi: 10.1007/s11434-009-0019-4

Zhou, F., Huang, D., Xue, H., Xuan, J., Yan, T., Ni, X., et al. (2017). Circulations associated with cold pools in the bohai Sea on the Chinese continental shelf. *Cont. Shelf Res.* 137, 25–38. doi: 10.1016/j.csr.2017.02.005

Zou, L., Zhang, J., Pan, W. X., and Zhan, Y. P. (2001). *In situ* nutrient enrichment experiment in the Bohai and Yellow Sea. *J. Plankton Res.* 23, 1111–1119. doi: 10.1093/plankt/23.10.1111